Project 1: The Role of PTPN22.6 in Intermediate Uveitis

Supervisors: Dr. Graham Wallace

Project 2: Cord Blood Mononuclear Cells as an Alternative Source for Chimeric Antigen Receptor-mediated Cancer Immunotherapy

Supervisors: Dr. Steve Lee and Dr. Frederick Chen

By

Vanessa Tubb

A thesis submitted to the University of Birmingham for partial fulfilment of the degree of Master of Research

College of Medical and Dental Science

University of Birmingham

October 2013

Abstract

BACKGROUND:

Uveitis, an inflammatory disease with a putative autoimmune component, is a major cause of visual impairment in the UK. Lyp is a protein tyrosine phosphatase encoded by the gene PTPN22 which dampens TCR signalling. Mutations in PTPN22 are associated with autoimmune susceptibility. PTPN22.6 is a novel Lyp isoform suggested to correlate with rheumatoid arthritis. The role of this variant in uveitis pathology is therefore intriguing.

METHODS:

Jurkat and CD4-T cells isolated from healthy and intermediate uveitis (IU) patients were stimulated using anti-CD3 and anti-CD28 antibodies. Lyp expression was detected by western blot and real-time quantitative PCR (rt-qPCR) in parallel. Expression of full-length PTPN22.1 and PTPN22.6 was determined in healthy and IU whole blood by rt-qPCR.

RESULTS:

Jurkat and CD4-T cells expressed multiple Lyp isoforms which increased after TCR stimulation. Full-length Lyp was most abundant in healthy patients, whereas smaller isoforms dominated in IU patients after stimulation. PTPN22.6 expression was detectable in all cells but variation was seen between healthy patients. Expression of PTPN22.1 and PTPN22.6 was not statistically different between control (n=26) and IU (n=39) patients, however interestingly the .1/.6 ratio was higher in control patients.

CONCLUSIONS:

The balance between Lyp isoforms may alter T cell responsiveness and be important in IU.

Table of Contents

1.0 INTRODUCTION

1.1 Autoimmunity

The purpose of the immune system is to efficiently recognise and remove foreign pathogens from the body before they cause disease. Specific pathogen recognition occurs through unique receptors on the surface of lymphocytes termed T and B cell receptors (TCR/BCR). TCR/BCR diversity allows recognition of a plethora of antigens including self-antigens (Janeways, 2008). Conditioning the immune system to be tolerant of self is essential for the prevention of autoimmune disease, although these mechanisms are not fool-proof (Gregersen *et al*, 2006). The initiation of autoimmunity is complex and is due to a failure in multiple immunological tolerance checkpoints that usually override self-reactivity. In addition, it has been well documented that environmental factors and epigenetic changes influence the propagation of autoimmune pathogenesis (Goodnow, 2007).

1.2 Lymphoid Protein Tyrosine Phosphatase

1.21 Protein Tyrosine Phosphatases and T cell Activation

When a TCR encounters cognate antigen, displayed by major histocompatability complexes (MHC), proximal TCR signalling events shown in Figure 1 are triggered. This results in the activation and differentiation of T cells into functional effector subsets (Burn *et al*, 2011). Protein tyrosine phosphatases (PTPs) are catalytic enzymes that coordinate the activity of cell signalling intermediates by dephosphorylating inhibitory and activatory tyrosine residues. The lymphoid PTP Lyp is a cytoplasmic PTP that negatively regulates T cell activation by interacting with multiple members of the Src and Syk family kinases.

Figure 1|TCR Signalling Interactions (Burn *et al*, 2011). Lyp negatively regulates many substrates involved in downstream TCR signalling by dephosphorylating tyrosine residues, as shown by the red lines. Lyp is also thought to itself be regulated by the positive signalling intermediate Lck.

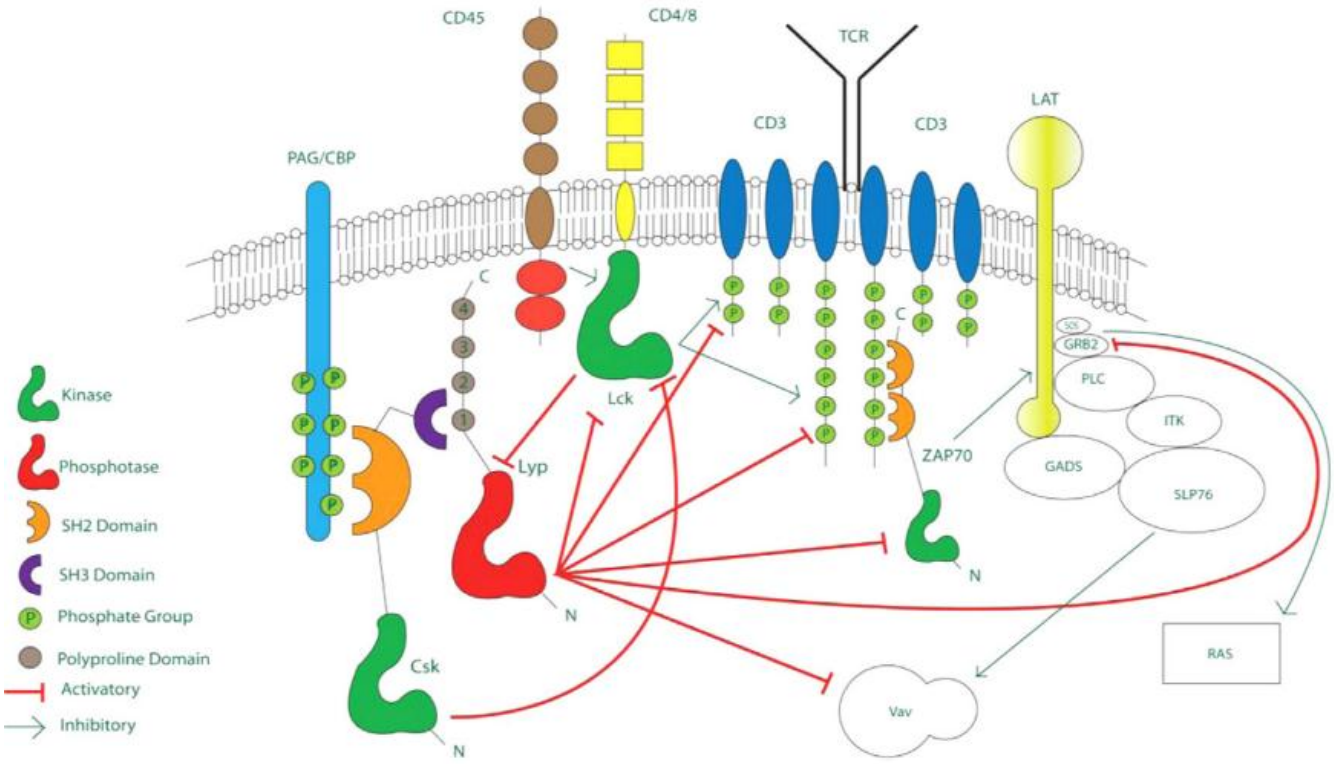

Substrate trapping experiments created by Flint *et al* (1997), have identified many Lyp substrates in this pathway including the positive signalling intermediates Lck, ZAP70, Vav1, Grb2 and c-Cbl. Lyp is exclusively expressed in haematopoietic cells, most abundantly in neutrophils and natural killer cells and less so in lymphocytes and monocytes, therefore its activity is pivotal in the regulation of the whole immune response (Burn *et al*, 2011), (Arimura, Y. & Yagi, J. 2010).

1.22 Lyp Protein Isoforms

Lyp consists of 3 domains: an N-terminal catalytic domain where it physically interacts with substrates, an interdomain, and a C-terminal domain consisting of 4 proline-rich motifs (Cohen *et*

al, 1999). Lyp is encoded by the protein tyrosine phosphatase non-receptor type 22 (PTPN22) locus on chromosome 1p13.3–13.1, which has been found to produce many alternatively spliced transcripts giving rise to different protein isoforms. Most abundantly found in immune cells is the full length protein designated Lyp 1 (105KDa). Other Lyp isoforms including Lyp 2 (85KDa), which does not contain a C-terminal domain, and Lyp 3 (779aa), containing a deletion in exon 15, have been shown to be present in peripheral blood mononuclear cells (PBMCs) (Wang *et al*, 2010). The functions of these isoforms have not yet been revealed, however Ronninger *et al* (2012) reported a direct change in the PTPN22 transcript profile under proinflammatory conditions, indicating a potential role for PTPN22 isoforms in handling inflammation. (Burn *et al*, 2011). The expression of Lyp in Jurkat cells, a T cell lymphoma cell line, was investigated by Chang *et al* (2012). They detected multiple Lyp isoforms by probing cell extracts with an anti-Lyp antibody. On transfection with small interference RNA (siRNA) against PTPN22, several protein bands were reduced suggesting that these isoforms are either Lyp1 degradation products or alternative splice variants.

1.3 PTPN22 and Autoimmune Disease

1.31 PTPN22 Susceptibility Mutations

In 2004 the C1858T SNP was linked to autoimmune type 1 diabetes (T1D) within two separate populations (Bottini *et al*, 2004). A single base-pair mutation in the PTPN22 gene at position 1858 of cytosine to thymidine (C1858T), results in the substitution of arginine to tryptophan at codon 620 (R620 to 620W). This data provided the first evidence of Lyp's role in autoimmune disease, and since then the C1858T SNP has been strongly and reproducibly linked to many other autoimmune diseases including rheumatoid arthritis (RA), Hashimoto's thyroiditis, Grave's disease, Addison's disease and Myasthenia Gravis, (Burn *et al*, 2011). The clustering of core autoimmune

diseases suggests that the breakdown of the immunological tolerance pathway involving PTPN22 is common to these conditions (Criswell e*t al*, 2005).

1.32 R620W Variant Function

As Lyp is a gatekeeper of T cell activation, it seems plausible that a SNP in this protein could alter TCR signalling threshold and allow maturation and activation of potentially harmful T cells, therefore predisposing to autoimmunity. However, whether the C1858 SNP is a gain- or loss- of inhibitory function mutation is debated. Vang *et al* (2005) found 620W Lyp to be more efficient at dephosphorylating proteins in the early TCR signalling pathway compared to R620 Lyp, suggesting C1858T SNP to be a gain-of-function mutation. This alteration in TCR signalling threshold may allow the escape of autoreactive T cells with high affinity for self-peptides, from being deleted during negative selection in the thymus. Similarly, the conversion of regulatory T cells within the thymus may be reduced contributing to autoimmune susceptibility. Conversely, Begovich e*t al* (2004) studied the effect of siRNA on Lyp function within the Jurkat T cell lymphoma cell line and found that knocking down Lyp resulted in increased TCR signalling by two-fold when compared to normal Jurkat cells.

Another hypothesis is that the change in Lyp expression is due to calpain 1-mediated degradation. Calpains are calcium-dependent proteolytic enzymes ubiquitously expressed in all cells that are capable of cleaving PEST-motif–containing proteins such as Lyp. Zhang *et al* (2011) have shown evidence for increased Lyp degradation in mice expressing the murine autoimmune Lyp variant Pep619W compared to wild-type Pep619R mice. Although Lyp transcript levels were similar between mice, immunoprecipitation of cell lysates with Pep antibody showed a significantly reduced level in Pep619W mice. Binding and cleavage assays revealed that Pep619W and Pep619R

could bind calpain and were cleaved by it; however the variant Pep619W bound more strongly to calpain and was therefore degraded rapidly.

Research by Brownlie *et al* (2012) has shown the effect of PTPN22 on immunosuppressive T regulatory cells (Treg). PTPN22 knock-out Tregs were found to be more immunosuppressive in an autoimmune colitis mouse model and controlled disease better compared to Tregs with functional PTPN22. In addition it was seen that PTPN22 knock-out Tregs secreted more of the anti-inflammatory cytokine IL-10 and had enhanced adhesive properties, but did not appear to affect their downstream TCR signalling.

Although it is accepted that Lyp functions as a negative regulator of TCR signalling, the controversy over the function of mutant Lyp is on-going and needs to be dissected in order to fully understand its role in autoimmune pathogenesis.

1.33 620W and Ethnicity

The frequency of 620W varies between ethnic groups. The distribution of the C1858T SNP resides mainly within Europe, with the highest allelic frequency in the most north-easternly countries and a frequency decreasing towards more south-westernly countries (Figure 2) (Burn *et al*, 2011). Although the allele is robust in the Caucasian population, the mutation is extremely rare in Asian and African populations as confirmed by multiple large cohort genetics studies (Kawasaki *et al*, 2006). It has been suggested that the mutation might persist in the Caucasian population due to selective advantages against certain infections including Tuberculosis (Lopez-Escamez, 2010). It is also hypothesised that other alternative PTPN22 SNPs may be present within Asian and African populations (Gregersen *et al*, 2006). No differences in disease pathology are seen between 620W Caucasian autoimmune patients and R620 Asian autoimmune patients. This could mean a different mutation in PTPN22, or another molecule involved in tolerance mechanisms, may be

contributing to autoimmunity in those parts of the world. A reason for this potential difference could be due to selection pressures to regional pathogens.

Figure 2|The Geographical Frequencies of the C1858T SNP (Gregerson *et al*, 2006). This map shows the average frequencies of the C1858T SNP throughout Europe, with an obvious decline in frequency from north-west to south-east.

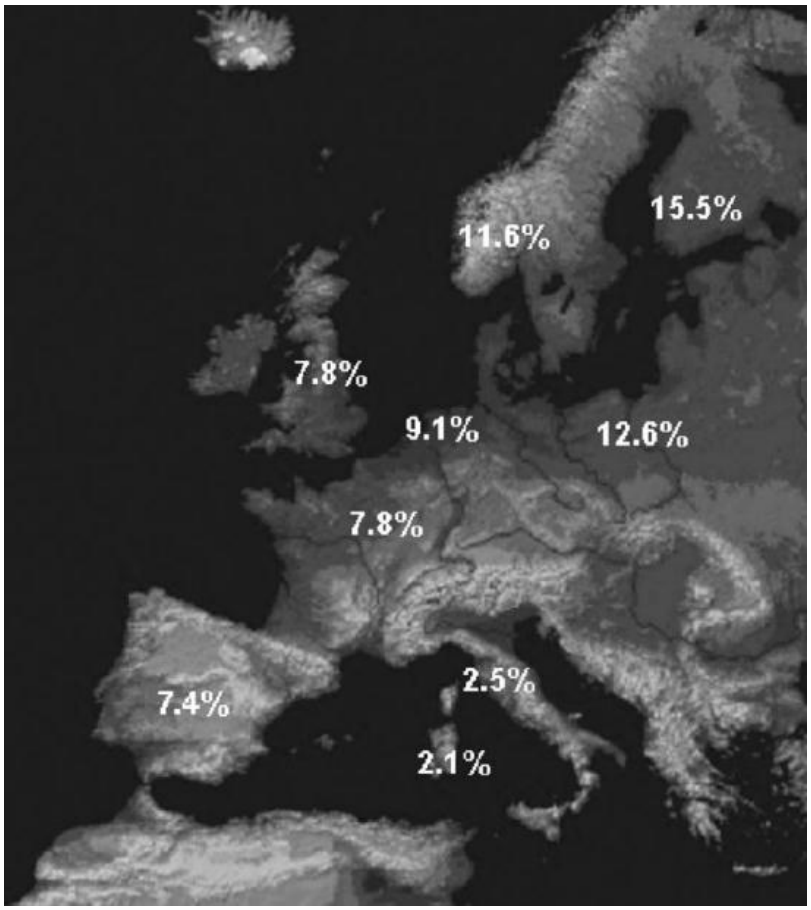

1.34 PTPN22.6

Last year Chang *et al* (2012) discovered an alternative splice form of PTPN22 designated PTPN22.6. This isoform lacks nearly the entire phosphatase domain and exon 21, however included a novel 8 amino acid sequence giving rise to a protein of 76KDa (Figure 3). They were able to confirm the presence of the PTPN22.6 transcript in human CD4+ T cells that were stimulated *in vitro* using anti-CD3 and anti-CD28 monoclonal antibodies using real-time PCR. In order to ensure the PTPN22.6

protein reported was not merely a degradation product of full-length PTPN22, siRNA was used to knock-down PTPN22. On addition of siRNA, no protein band corresponding to the 76KDa PTPN22.6 protein was visible; therefore the isoform is an alternative splice product rather than a fragment of PTPN22. Forced expression of R620 or 620W PTPN22.1 or PTPN22.6 isoforms within primary human CD4+ T cells, revealed that both R620 and 620W PTPN22.1 decreased IL-2 production from T cells in a dose-dependent manner. Interestingly, 620W PTPN22.6 enhanced IL-2 production also in a dose-dependent manner 20-30% more than R620PTPN22.6, thus suggesting the presence of mutant PTPN22.6 could account for hyperactivity of T cells and pathogenesis in autoimmune disease. Most importantly and clinically relevant was the finding that PTPN22.6 expression in peripheral blood was associated with disease activity in RA patients (Chang *et al*, 2012).

The frequency of PTPN22 splice variants in PTPN22-associated autoimmune disease has been investigated by Ronninger *et al* (2012). The mRNA expression of the PTPN22 splice variants Lyp1 and Lyp 2 in unstimulated peripheral blood mononuclear cells (PBMCs) were investigated in 3 independent cohorts of RA and control patients that were also genotyped for the C1858T polymorphism. They reported a higher expression of the longer isoform Lyp1 and a lower expression of the shorted isoform Lyp2 within RA patients when compared to controls. However, this was found to not be associated with any polymorphisms in the PTPN22 locus.

Figure 3|A Diagram Representing the PTPN22 Gene and its Alternatively Spliced Variants (Chang *et al*, 2012). PTPN22 encodes the protein Lyp and can be alternatively spliced to produce different isoforms. PTPN22.1 denoted the largest full-length Lyp protein; however PTPN22.6 lacks most of the PTP catalytic domain (exons 4-10) due to alternative splicing.

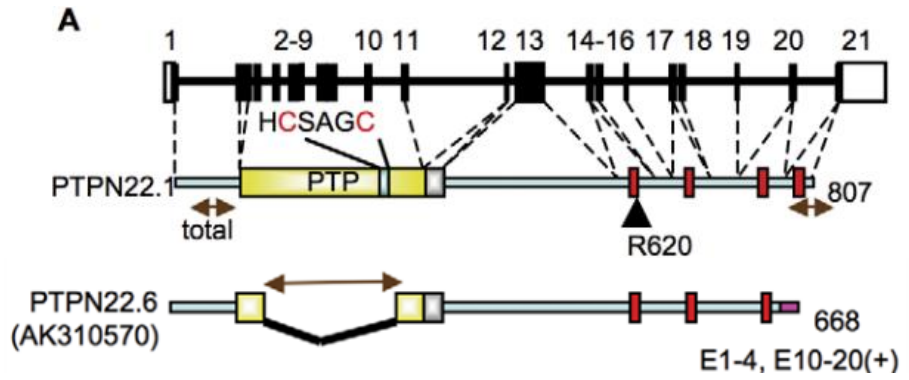

1.4 Autoimmune Uveitis

1.41 What is Uveitis?

Uveitis is the generalised inflammation of the uvea: the middle layer of the eye which consists of the choroid, ciliary body and iris. The eye is very delicate and is normally a site of immune privilege; however during attacks of inflammation vision can be compromised. Uveitis is a destructive and limiting disease which accounts for a majority of legal blindness in the UK (Caspi, 2010). It primarily afflicts young adults (20-50 years of age) who are in their most prolific years, consequently creating both a personal and economic burden (Chang *et al*, 2005). Uveitis can be caused by infectious agents such as cytomegalovirus (CMV), however most cases of uveitis are termed non-infectious, immune-mediated uveitis, and are caused by aberrant immune responses to self-antigens (Caspi, 2010). There are 3 anatomical classifications of uveitis within the eye: anterior, intermediate and posterior, or pan uveitis which refers to inflammation of both the anterior and posterior of the eye. Uveitis may exist as a disease on its own but may also present as part of a systemic autoimmune condition such as in Behçet's disease and ankylosing spondylitis

(Babu & Rathinam, 2010). Visual impairment is a serious disability; therefore research into the pathology of uveitis is one of great importance.

1.42 Pathology of Autoimmune Uveitis

The intraocular environment is unique in that it contains a high level of immunoinhibitory cytokines such as TGF-β. The physical separation of the eye from the immune system by the blood-retinal barrier also limits local inflammatory responses. These mechanisms mean the eye does not experience immune damage from day-to-day pathogenic insults. Expression of retinal antigens such as retinal arrestin and interphotoreceptor retinoid–binding protein (IRBP) within the thymus is necessary for immune tolerance, as mice deficient in the AIRE gene develop ocular pathology (Anderson *et al*, 2002). The etiology of autoimmune uveitis has been closely linked to immune responses directed against retinal antigens such as uveal melanin and proteins involved in its metabolism. Immunising mice with T cells specific for retinal antigens has enabled the development of experimental autoimmune uveitis (EAU) animal models and has consequently highlighted the autoimmune element of uveitis. It is thought that autoimmune uveitis is linked to pathogenic insult and activation of the innate immune system resulting in a sustained immune response to self-antigens in the same environment (Read, 2006).

1.43 Genetic Associations of Uveitis

Acute anterior uveitis (AAU) is strongly associated with the HLA (human leukocyte antigen)-B27 haplotype (Chang *el al,* 2005). AAU is the most common subtype of uveitis among most of the world's population, accounting for 92-50% of uveitis cases in the western world but only 28-50% in Asia. In the western world, 18-32% of AAU patients are HLA-B27 positive, with 6-13% of AAU patients in Asia showing a degree of variation between ethnic groups. In addition there is a clear male predominance with males being affected between 1.5 to 2.5 times more often than females.

A strong association of HLA-B27 with generic inflammation has been known since 1973 and is still one of the strongest HLA-disease associations; however the complex mechanism by which this haplotype contributes to pathology remains unknown (Chang *et al*, 2005). Other weaker genetic associations with AAU have been reported, such as the TNF−857T allele (Kuo *et al*, 2005) and the C4B2 allotype (Wakefield *et* al, 1988), however no associations were found between the R620W SNP within the PTPN22 gene and the prevalence of AAU in a large patient cohort from Portland, USA (Martin *et al*, 2009). Uveitis is one of many multifactorial autoimmune diseases that have a genetic predisposition as well as an environmental influence. Susceptibility loci are likely to be a common link between autoimmune diseases as a whole. A study performed by Mattapallil *et al* (2008), found both protective and disease associated quantitative trait loci that colocalised with other models of uveitis and human disease-modifying loci in a rat animal model of EAU. Although no associations have currently been found between PTPN22 and the incidence of uveitis, considering the association of the R620W SNP to a large number of autoimmune disease, other unknown PTPN22 modifications are likely to contribute to uveitis disease severity.

1.5 Aims

- To analyse the expression of Lyp protein within resting Jurkat cells and primary CD4+ T cells isolated from healthy and intermediate uveitis (IU) donor peripheral blood, and how activation of these cells with anti-CD3 and anti-CD28 antibodies affects Lyp protein expression.
- To determine the relative transcript levels of PTPN22 isoforms within resting and activated Jurkat and healthy and IU donor CD4+ T cells, and healthy and IU whole blood DNA samples.

1.6 Hypothesis

I hypothesise that Jurkat and primary CD4+ T cells will express multiple Lyp isoforms of varying sizes, but will express full-length Lyp most abundantly. It is expected that Lyp expression will increase in response to TCR stimulation but to a lesser degree in CD4+ T cells from IU patients. Finally, I expect to see a correlation between the frequencies of PTPN22.1 and PTPN22.6 and IU.

2.0 MATERIALS AND METHODS

2.1 Table of Reagents and Medias

Reagent or Media	Ingredients
Complete RPMI	RPMI (Roswell Park Memorial Institute) 1640 [Gibco, UK], 1% GPS (2Mm L-glutamine, 100U/ml penicillin, 100µg/ml streptomycin) 10% Heat Inactivated Fetal Calf Serum (HIFCS) [Biosera, Ringmer, UK]
Phosphate buffered saline (PBS)	Prepared by 1 PBS tablet per 100ml ionised H20 [Oxoid, Basingstoke, UK]
RIPA lysis buffer	0.5M Tris-HCl, pH 7.4, 1.5M NaCl, 2.5% deoxycholic acid, 10% NP-40, 10mM ethylenediamine tetra-acetric acid (EDTA) [Millipore]
AutoMACS separation buffer	PBS, bovine serum albumin (BSA), EDTA, 0.09% azide, pH 7.2 [Miltenyi Biotec]
NuPAGE MOPs running buffer	50 mM MOPS, 50 mM Tris Base, 0.1% SDS, 1 mM EDTA, pH 7.7 [Novex, Life technologies]
TBS-tween	10mM Tris-HCl, 100nM NaCl, 0.1% Tween-20 [Sigma-Aldrich], pH 7.5
Stripping Buffer	15g glycine, 1g SDS, 10ml Tween-20, 1L ionised H20, pH 2.2
1X TBE Buffer	0.089M Tris, 0.089M borate, 2mM EDTA, pH 8.3 [Invitrogen]

2.2 Patient Samples

Blood was collected from Caucasian healthy control patients and IU patients from the Birmingham and West Midland Eye Centre. Patients had given informed consent based on approval by the local Ethics Committee. DNA was isolated from whole blood using the desalting method and diluted to a concentration of 20pg/µl and stored in 96-well plates at 4°C. These patient samples were part of the Genetic Polymorphisms in Uveitis study.

2.3 Cell Isolations and Cell Culture

Jurkat cells were cultured in complete RPMI at 37°C 5% CO_2 in a T75 flask [Sarsteadt], and passaged every 4 days. Human blood was collected in EDTA-treated vials and diluted 1:1 with

complete RPMI. Peripheral blood mononuclear cells (PBMCs) were isolated via Ficoll-paque [GE Healthcare] gradient centrifugation for 30 minutes (4000G, 20°C, brake 0) and washed twice by centrifuging for 8 minutes (300G, 20°C), removing the supernatant and resuspending cells in complete RPMI. CD4 microbeads [Miltenyi Biotec] were used to positively isolate CD4+ T cells from PBMCs according to the manufacturer's instructions. AutoMACS cell separation buffer was purchased from Milenyi Biotec. Where possible, $1x10^6$ CD4 T cells or Jurkat cells in 1ml of complete RPMI were cultured in 24-well cell culture plates at 37°C, 5% CO_2. CD4 T cells and Jurkat cells were stimulated using 2.5µg/ml of plate-bound anti-CD3 antibody [R&D, HIT3a] and 2.0µg/ml of soluble anti-CD28 antibody [R&D, CD28.2] in the presence of IL-2 (50U/ml)[Immunotools, #352593] for 0, 1, 3, 5 or 7 days at 37°C, 5% CO_2.

2.4 Western Blotting

The expression of functional Lyp protein in cell lysates was studied by western blot.

2.41 BioRad Protein Assay

Cells were lysed using an appropriate amount of RIPA lysis buffer [Upstate, Millipore], based on the size of the cell pellet, for 10 minutes and stored at -20°C until ready for analysis. The protein concentration in cell lysates was analysed using the BioRad colorimetric protein assay [BioRad Laboratories, UK] compared to standard concentrations of BSA [Sigma] and measured by reading the absorbance at 595nm on a Biotek synergy spectrophotometer (Figure 1).

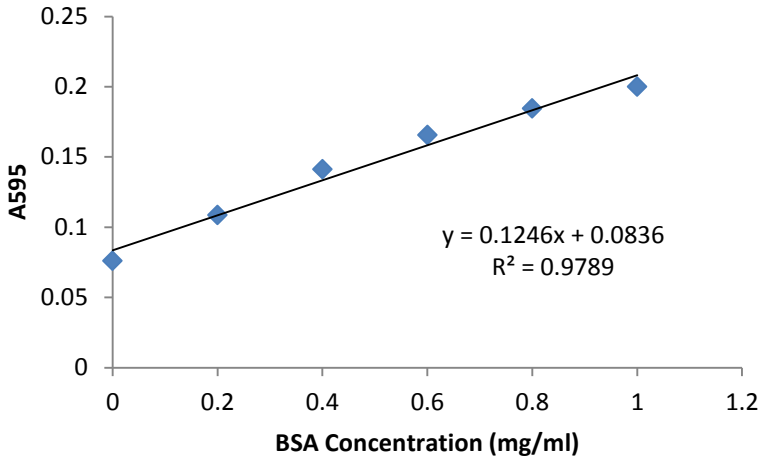

Figure 1: An example of a BioRad protein assay standard graph showing A_{595} Vs BSA concentration (mg/ml).

Cell lysates were prepared in reducing NuPAGE western blot reagents [Novex, life technologies] according to the manufacturer's instructions and boiled at 70°C in a water bath for 10 minutes to denature proteins. 20µg of protein (where possible) was resolved by electrophoresis on NuPAGE 4-12% Bis-Tris 1.5mm precast mini gel cassettes [Novex, life technologies] in a cell-lock mini electrophoresis tank [Invitrogen] for 60 minutes at 200 voltage and 150 current. The chambers of the electrophoresis tank were filled with NuPAGE MOPS running buffer [Novex] with the addition or 500µl of antioxidant [Novex] to the inner chamber. Mini gels were then transferred to mini Trans-blot Turbo transfer 0.2µm polyvinylidene difluoride (PVDF) membranes [BioRad] using the BioRad Trans-blot turbo transfer system. The membrane was then blocked in 5% milk solution for 60 minutes at room temperature.

Proteins were detected using specific antibodies diluted in 5% milk solution at the manufacturers recommended concentrations (Table 1). The membrane was incubated in primary antibody overnight at 4°C and then washed three times in TBS-tween for 5 minutes on a plate shaker. The secondary HRP-conjugated antibody was then added to the membrane and incubated for 60 minutes at room temperature on a plate shaker. The chemiluminescent substrate Advance ECL

[Amersham, GE Healthcare] was used for detection of antigen-antibody complexes according to manufacturer's instructions. Chemiluminescence was then detected on a Chemi-Doc imager [BioRad]. The membrane was washed three times in TBS-tween for 5 minutes before being mildly stripped by washing twice for 10 minutes in stripping buffer, twice for 10 minutes in PBS and finally twice for 5 minutes in TBS-tween. The stripping of the membrane was needed to re-probe for a loading control, in this case β-actin. The membrane was then re-blocked in 5% milk powder for 60 minutes.

Table 1: List of Antibodies used for Western Blotting

Name	Company	Clone Number	Catalogue Number	Concentration
Human anti-Lyp goat IgG	R&D Systems	XMR0112041	AF3428	1:500
HRP-conjugated goat IgG	R&D Systems	XGDO612041	HAF109	1:1000
Anti-beta actin- loading control	Abcam	P60709	Ab8227	1:1000
HRP-conjugated anti-rabbit IgG	GE Healthcare, Amersham	N/A	NA934	1:5000

2.5 Polymerase Chain Reaction (PCR)

Real-time PCR was used to study Lyp isoform gene expression.

2.51 RNA Extraction and cDNA Synthesis

RNA was extracted from cell pellets using an RNeasy mini kit [Qiagen] following the manufacturer's instructions. RNA was quantified by spectrometry at 260nm [Thermoscientific Labtech] and the purity checked by measuring the A_{260}/A_{280} ratio. 1µg of RNA was converted to cDNA using the enzyme reverse transcriptase. cDNA synthesis was performed in 11µl of 2.5Mm NaCl [Applied Biosystems], 5µl of 10X reverse transcriptase buffer [Applied Biosystems], 10 µl of 10mM dNTP mix [Applied Biosystems], 3.2 µl of 50U/µl multiscribe reverse transcriptase [Applied

Biosystems], 2.5µl of 5mM random hexamer primers [Applied Biosystems] and 1µl of 20U/µl RNase inhibitor [Applied Biosystems]. The reaction mixtures were made up to 50µl with RNAse-free water and heated to 25°C for 10 minutes, 37°C for 60 minutes, 48°C for 30 minutes and 95°C for 5 minutes using a T100 thermal cycler [BioRad].

2.52 Conventional PCR

PCR primer sequences for Total PTPN22, PTPN22.1, PTPN22.6 and β-actin were obtained from Chang *et al* (2012) and purchased from integrated DNA technologies (Table 2). Conventional Taqman PCR was performed to assess the PCR primer specificities. Primers were reconstituted in sterile PBS at a concentration of 25 nM. RNA was extracted from naïve Jurkat cells and converted to cDNA as described above. A PCR mastermix was made containing 9.8µl of RNase free water, 4µl of RB 5X buffer [Applied Biosystems], 1.6µl of 25mM $MgCl_2$ [Applied Biosystems], 0.5µl of dNTP's [Applied Biosystems], 0.1µl of GoTaq polymerase [Invitrogen], 1µl of forward primer and 1µl of reverse primer per sample. 2µl of cDNA was added to 18ul of mastermix and run on a BioRad T100 thermal cycler at the following temperatures: 94°C for 5 minutes (1 cycle), 94°C for 30 seconds, 60°C for 30 seconds, 72°C for 30 seconds (33 cycles) and 72°C for 7 minutes (1 cycle). Electrophoresis on agarose was performed to resolve PCR products. An agarose gel was made using 1.5g of agarose [Invitrogen] in 75mls of TBE buffer and 0.75µl of ethidium bromide. 15µl of either sample or DNA ladder was loaded into wells in the agarose gel and the gel was run at 80V, 115 current for 50 minutes. The gel was then imaged on a Chemidoc imager [BioRad].

2.53 Real-time PCR

Brilliant III ultra-fast SYBR Green QPCR master mix [#600828, Stratagene] was used for real-time PCR according to manufacturer's instructions. 2µg of cDNA or 100pg of patient DNA was added to individual wells of a 96-well semi-skirted PCR plate with 19µl of master mix and mixed gently to

avoid forming bubbles. All real-time PCR reactions were performed on a Stratagene Mx3000P qPCR machine using temperatures and cycles taken from Chang *et al* (2012). The value at which the fluorescence emitted by SYBR green goes about the threshold is the Ct value (cycle threshold) and determines the amount of fluorescence emitted in each primer reaction and therefore gene quantification in relation to β-actin.

Table 2: Oligonucleotide Sequences of PCR primers

Gene	**Forward Primer (5' to 3')**	**Reverse Primer (5' to 3')**	**Product Size (base pairs)**
Total PTPN22	GCAGAAGTTCCTGGATGAG	TCAGCCACAGTTGTAGGATAG	129
PTPN22.1	TGCCCACCAAACAAGCC	TGGTGGTGGATTCCTTGG	111
PTPN22.6	TTTGCCCTATGATTATAGCCG	GTTCTCAGGAATTATAAGGACACT	197
β-actin	GTGACAGCAGTCGGTTGGAG	AGGACTGGGCCATTCTCCTT	176

2.6 Statistical Analysis

A two-tailed unpaired t-test was used to determine the difference in PTPN22 transcript levels between healthy and IU patients. Statistical significance was reached when $P \leq 0.05$.

3.0 RESULTS

3.1 Lyp Expression within Jurkat Cells

Lyp is a damper of TCR signalling and has previously been identified exclusively in haematopoietic cells. Jurkat cells are a T cell lymphoma cell line used to study T cell behaviour *in vitro*. Following on from work by Chang *et al* (2012), Lyp expression was first investigated within Jurkat cells because as a cell line preliminary experiments are repeatable. Jurkat cells were cultured in complete RPMI and subjected to cell lysis and western blotting (Figure 1a). In naïve jurkat cells a total of 7 Lyp protein species were detected using an anti-Lyp IgG antibody. The largest molecular weight species was detected at around 105kDa corresponding to full length Lyp that is expressed most abundantly in haematopoietic cells (Burn *et al*, 2011). The most prominent band was found at 80kDa which may correlate with the Lyp 2 isoform suggested to be 85KDa, however this would disagree that Lyp 1 is the most abundant isoform. 5 other lower molecular weight Lyp species were also detected around 57kDa, 48kDa, 44kDa, 32kDa and 18kDa. PTPN22.6 was found to have a molecular weight of 76kDa, however a band was not detected at this molecular weight.

3.2 Lyp Expression Following Jurkat Cell Stimulation

After multiple Lyp species were found in resting Jurkat cells, we next investigated what happened to Lyp expression after stimulation with plate-bound anti-CD3 and soluble anti-CD28 antibodies in the presence of IL-2 at various time points. Again Jurkat cells were lysed and their extracts subjected to western blotting with an anti-Lyp IgG antibody. It is clear that overall full-length Lyp (105KDa) expression increases after stimulation of Jurkat cells (Figure 1b). The expression of full-length Lyp continues to increase with an increasing length of T cell stimulation, however no Lyp 2 band at 80kDa as seen in Figure 1a was observed this time. Repeated experiments showed the

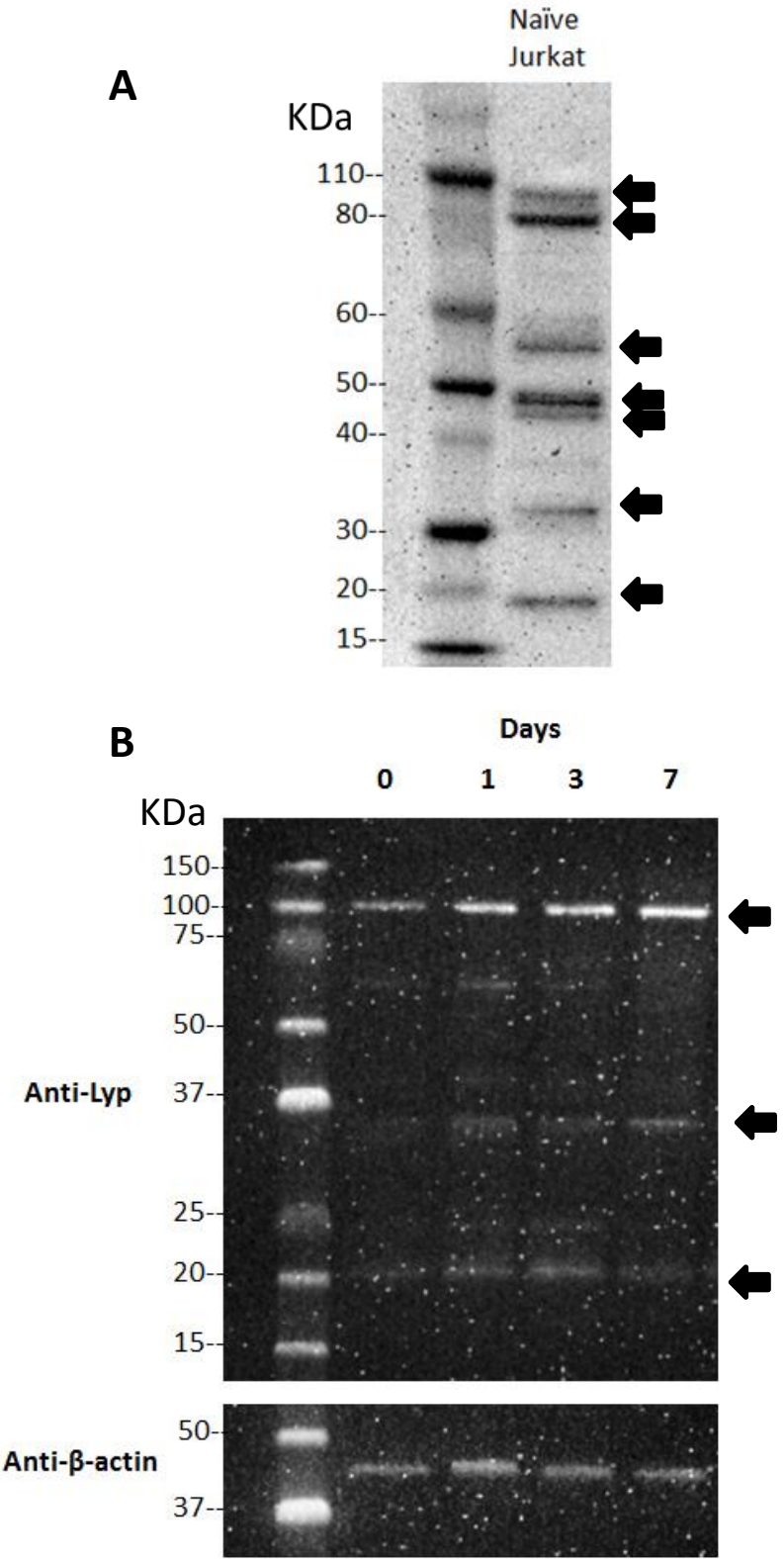

Figure 1| Lyp Expression in Resting and Stimulated Jurkat Cells. (A) Multiple Lyp protein species are detected by western blotting in resting jurkat cell lysate (n=1). (B) Changes in Lyp expression are shown after jurkat cell stimulation with anti-CD3 and anti-CD28 in the presence of IL-2 (n=2).

presence of a Lyp 2 band, however it was not possible at the time to perform β-actin loading controls and therefore results from these experiments were invalid.

Lower molecular weight Lyp products were again detected; however only two at around 35kDa and 21kDa are clear enough to visualise. These products are likely to be the same as those detected at around 32kDa and 18kD in Figure 1a. Although the β-actin loading control shows marginally less protein loaded at day 0, it is clear that smaller Lyp protein species are expressed at a higher concentration after TCR stimulation. 35kDa Lyp appears to reach maximal expression at day 7, whereas 21kDa Lyp expression peaks at day 5 and declines by day 7 but maintains a level higher than day 0. Lastly, there is no detection of a band at 76kDa relating to the new Lyp isoform PTPN22.6 even after cell stimulation, although we did not have a specific antibody for this isoform.

3.3 Lyp Expression in Primary Healthy and IU CD4+ T Cells

After CD4+ T cells were positively selected from PBMCs that were harvested from the peripheral blood of healthy and IU patients, cells were stimulated with anti-CD3 and anti-CD28 antibodies in the presence of IL-2 for a period of time and subjected to cell lysis and western blotting for Lyp. Similar patterns of Lyp expression are seen in healthy CD4 T cells as jurkat cells (Figure 2a). Full length Lyp could be detected at 105kDa, which peaks by day 5. Although β-actin expression is obviously lower in CD4+ T cells stimulated at days 0 and 1, a lower level of Lyp expression is still seen even after taking protein loading into account, suggesting Lyp production increases after stimulation. Multiple smaller Lyp species are also detected within CD4+ T cells around 60kDa, 35kDa, 25kDa and 20kDa, with again the most abundant isoform being full-length Lyp. The detection of these proteins is minimal; however their expression does appear to be maximal at day 5, as seen for full-length Lyp. Again there was no clear detection of a band matching the weight of PTPN22.6.

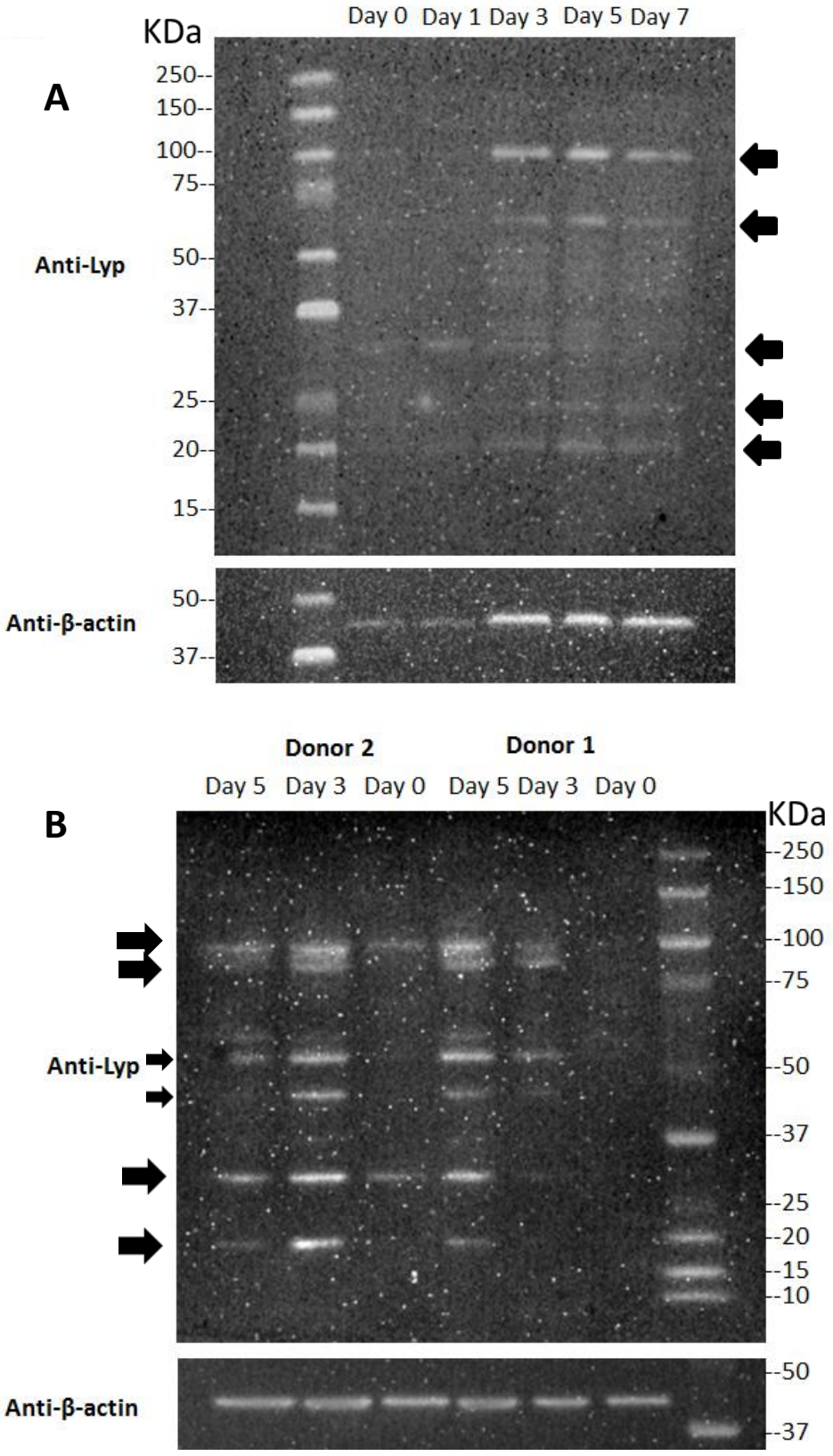

Figure 2| Lyp Expression within healthy and IU patient CD4 T cells. (A) Lyp expression is shown in CD4 T cells from a healthy patient stimulated over time (n=1). (B) Lyp expression is shown in CD4 T cells taken from 2 IU patients stimulated over time (n=1).

CD4+ T cells from two IU donors were stimulated for days 0, 3 and 5 only, due to having a limited number of cells, and analysed for Lyp expression (Figure 2b). No Lyp species were detectable in cells from donor 1 at day 0, most likely due to too a low protein concentration as we know all individuals express Lyp within their haematopoietic cells. Lyp protein expression increases by days 3 and 5 to a detectable level. Full-length Lyp is seen at 105kDa and again a slightly lower molecular weight band around 85kDa is seen corresponding Lyp 2. Smaller Lyp species are seen at 56kDa, 44kDa, 32kDa and 20kDa which are most abundant at day 5. Surprisingly the expression of 56kDa and 32kDa Lyp fragments was greater than that of full-length Lyp, which has so far been seen to be the most abundant. This observable difference between IU and healthy patients may therefore be important.

3.4 Total PTPN22, PTPN22.1 and PTPN22.6 Primers

Lyp gene expression was next explored to better understand its role in IU. Primer designs were retrieved from Chang *et al* (2012) to target β-actin, total PTPN22, PTPN22.1 and the novel PTPN22.6 genes. The PTPN22.1 primer targets full-length Lyp while the PTPN22.6 primer targets the PTPN22.6 variant derived from alternative splicing of PTPN22.1. The total PTPN22 primer was designed to target a 5' sequence shared by both PTPN22.1 and PTPN22.6, therefore in theory the level of PTPN22.1 and PTPN22.6 transcript should amount to that of total PTPN22. Conventional PCR was performed on resting jurkat cells to test the primer specificities as shown by their PCR product size (Figure 3). B-actin (176bps), total PTPN22 (129bps), PTPN22.6 (197bps) and PTPN22.1 (111bps) all appear as single bands at the correct corresponding length, confirming that the primers are specifically amplifying the correct DNA sequences. A negative control containing no primer sequences clearly shows no DNA amplification.

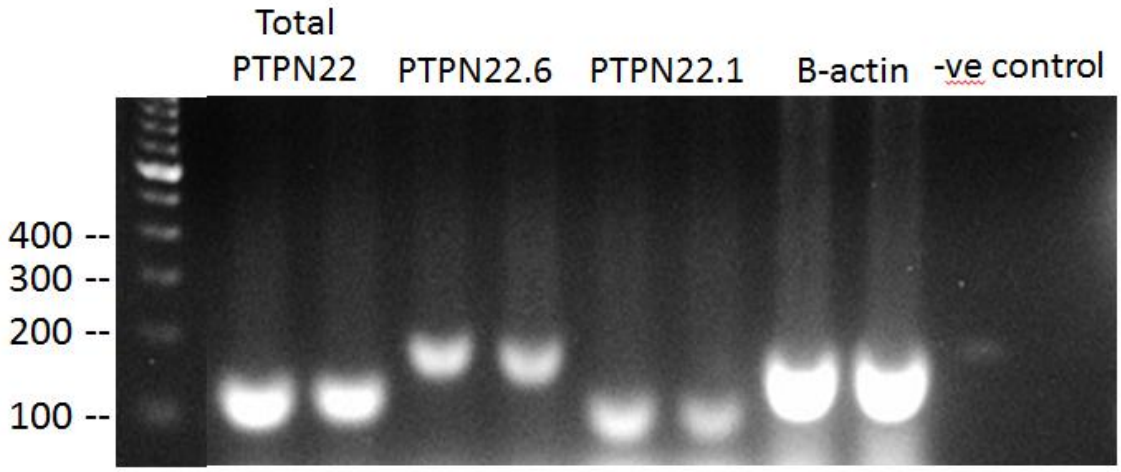

Figure 3| Testing designed primers using conventional PCR. β-actin, total PTPN22, PTPN22.6 and PTPN22.1 primers were analysed on jurkat cell lysates and PCR product sizes were measured in relation to a DNA base pair ladder (left). A negative control containing no primers was included n=1.

3.5 PTPN22 Expression in Jurkat Cells and Healthy and IU Patient CD4+ T cells

Jurkat cells and CD4+ T cells isolated from the blood of healthy and IU patients were stimulated as described previously. In parallel RNA was extracted from half of the cells and converted to cDNA for SYBR green real-time PCR experiments reproduced from Chang *et al* (2012). Total PTPN22, PTPN22.1 and PTPN22.6 gene expression was investigated in relation to β-actin expression. A consistent level of both total PTPN22 and PTPN22.1 transcript was seen in jurkat cells from day 0 to day 7 of stimulation (Figure 4). PTPN22.6 transcript was detectable in Jurkat cells following cell stimulation by day 1 which then declined to an undetectable level by day 5. Positive detection of this novel splice variant provides further evidence for its existence as was first shown by Chang *et al* (2012). It was expected that the total PTPN22 transcript level would increase marginally from days 1 to 5 in parallel with PTPN22.6, however this was not the case.

CD4+ T cells taken from three healthy donors were also subjected to real-time PCR. On average, the total PTPN22 transcript level was 0.55 on day 0 before cell stimulation, which went on to peak on day 3 at 0.7 after cell stimulation and decline by day 7 to 0.6. A similar pattern of mean PTPN22.1 expression was seen as expected because it is the dominant PTPN22 isoform, however data was not available on cells prior to stimulation on day 0 therefore the actual influence of cell stimulation on PTPN22.1 expression is unknown. Also of note is the complete decline of PTPN22.1 below a detectable level in healthy donor 2 by day 7. This value is likely to be an anomaly due to a low cDNA concentration as full length Lyp is always present within lymphocytes. PTPN22.6 transcript was detectable in all healthy donors at a relatively consistent level from day 1 to 7, with the exception of donor 3 who had twice the PTPN22.6 transcript expression by day 7 than donors 1 and 2. Of course variation was seen between the three healthy donors and as data for some time points was not available the mean values should be read with some caution.

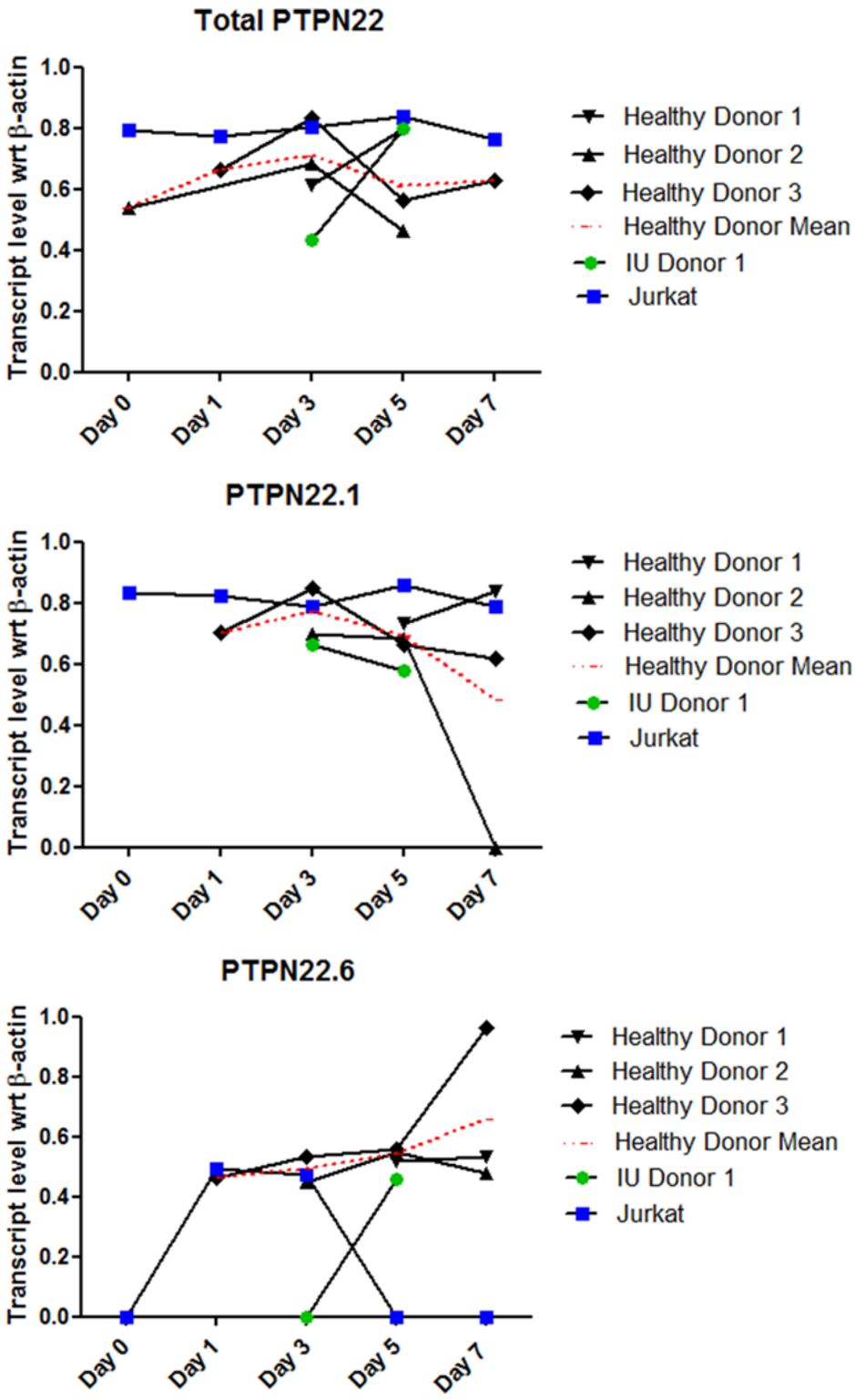

Figure 4| PTPN22 Gene Expression Within Jurkat cells and Healthy and IU Patient CD4 T cells Following Cell Stimulation. Total PTPN22, PTPN22.1 and PTPN22.6 transcript levels with relation to β-actin transcript levels were determined for 3 healthy donors, 1 IU donor and 1 jurkat sample.

CD4+ T cells from one IU donor were analysed for PTPN22 expression, however due to a limited cell number data could only be retrieved from days 3 and 5 of cell stimulation. On day 3 total PTPN22 expression was at a level comparable to healthy CD4 T cells before cell stimulation, which increased 2-fold to 0.8 by day 5. Although drawing conclusions from only two time points is almost impossible, it may suggest this IU donor had a delay in peak expression of total PTPN22 which was seen earlier at day 3 in healthy donors. PTPN22.1 expression was 0.7 on day 3 and 0.6 on day 5, seeming to follow a similar pattern as healthy donors but at a moderately lower level. PTPN22.6 expression was observed only on day 5 in the IU donor which could be the delayed result of cell stimulation.

3.6 PTPN22 Expression in Healthy Control and IU Patient Whole Blood DNA

26 healthy control patient and 39 IU patient whole blood DNA samples were analysed for total PTPN22, PTPN22.1 and PTPN22.6 gene expression in relation to β-actin also using SYBR green real-time PCR. Patient characteristics are shown in figure 5a. Over 50 control and IU patient samples were assessed for PTPN22 expression, however many results were excluded due to abnormal β-actin cT values or no detection of total PTPN22 transcript. Both IU and control samples expressed a comparable mean level of total PTPN22 (P=0.18), however there was a distinct population of IU patients with greater expression of total PTPN22 which could be due to factors including gender, age or ethnicity (Figure 5b). It was determined that both IU and control patients may or may not express PTPN22.1 or PTPN22.6 alongside total PTPN22 (Figure 5b). Mean expression of PTPN22.1 and PTPN22.6 was not significantly different between control and IU patients (P=0.31 and P=0.22 respectively), although PTPN22.6 expression was lesser than full-length PTPN22 in both groups. Some variation is clear amongst all patients for PTPN22 gene expression but this was to be expected. Additionally, total PTPN22 gene expression was similar to that observed for

A

	Total Number (n=)	Male (n=)	Female (n=)	Unknown Gender (n=)	Mean Age
Health Control Patients	26	5	14	7	30.4 +/- 8
IU Patients	39	15	23	0	55.6 +/- 15

B

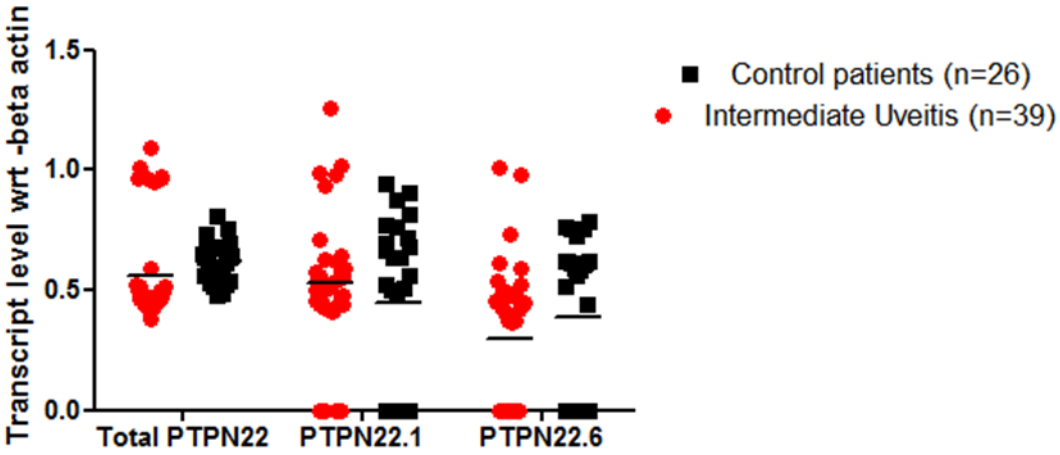

C

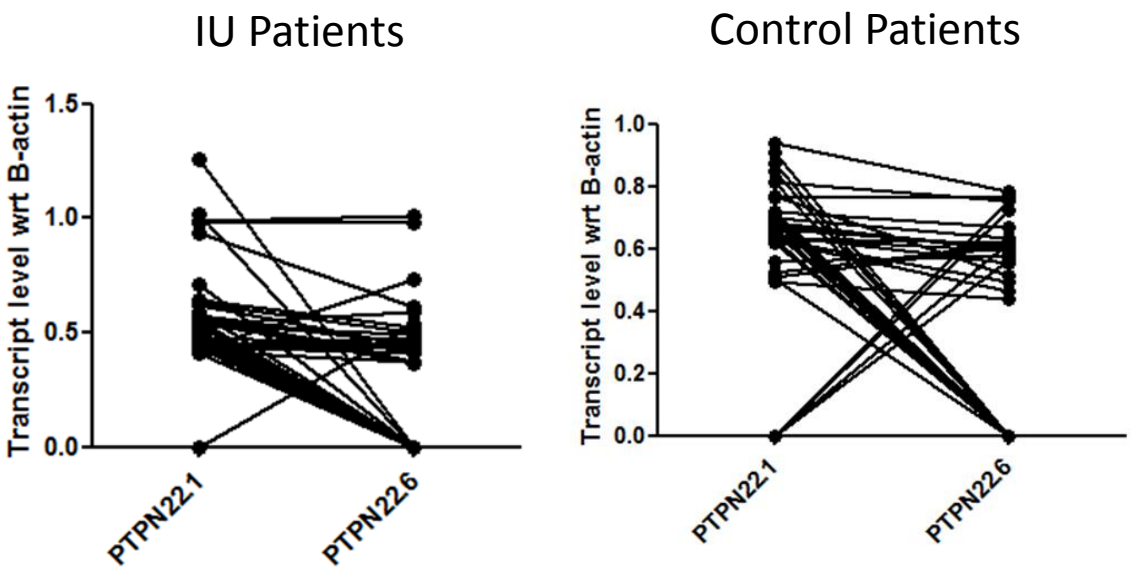

Figure 5| PTPN22 Gene Expression Analysis of IU and Control Patient DNA. The characteristics of the healthy control and IU patient groups are shown in A. The transcript levels of total PTPN22, PTPN22.1 and PTPN22.6, in relation to β-actin gene expression, for control and IU patients are shown in B. The relationships between PTPN22.1 and PTPN22.6 expression in IU and control patients are shown in C.

unstimulated healthy CD4 T cells (Figure 4), which could have been predicted as PCR was performed on DNA from unstimulated whole blood.

3.7 The Relationship between PTPN22.1 and PTPN22.6

Real-time PCR data has shown that either IU and control patients may express full-length PTPN22.1 or PTPN22.6 and be homozygotes, or they may express both isoforms and be heterozygotes. The relationship between PTPN22.1 and PTPN22.6 for each individual patient and the distributions of heterozygotes and homozygotes are shown in figure 5c. Although the heterozygous genotype was most frequent in both groups, just over 50% of control patients were heterozygous, compared to around only a quarter of IU patients. Furthermore, an almost equal number of PTPN22.1 and PTPN22.6 homozygotes were seen in control patients but only 1 PTPN22.6 homozygote was reported compared to 15 PTPN22.1 homozygotes in IU patients, indicating that the PTPN22.6 genotype is rarer in IU patients.

3.8 Gender Differences in PTPN22 Expression

Although many autoimmune diseases are more prevalent in females, uveitis affects males and females equally. However we wanted to determine whether gender influenced the level of expression of PTPN22 genes in IU and control patients (Figure 6). Although it was hypothesised that the distinct population of IU patients with greater total PTPN22 expression (Figure 5a) may be due to gender, it is clear that gender did not account for this finding as mean values for male and female total PTPN22 expression were nearly exact. In fact gender did not influence the expression levels of any PTPN22 genes in both control (Figure 6a) and IU patients (Figure 6b) ($P>0.05$).

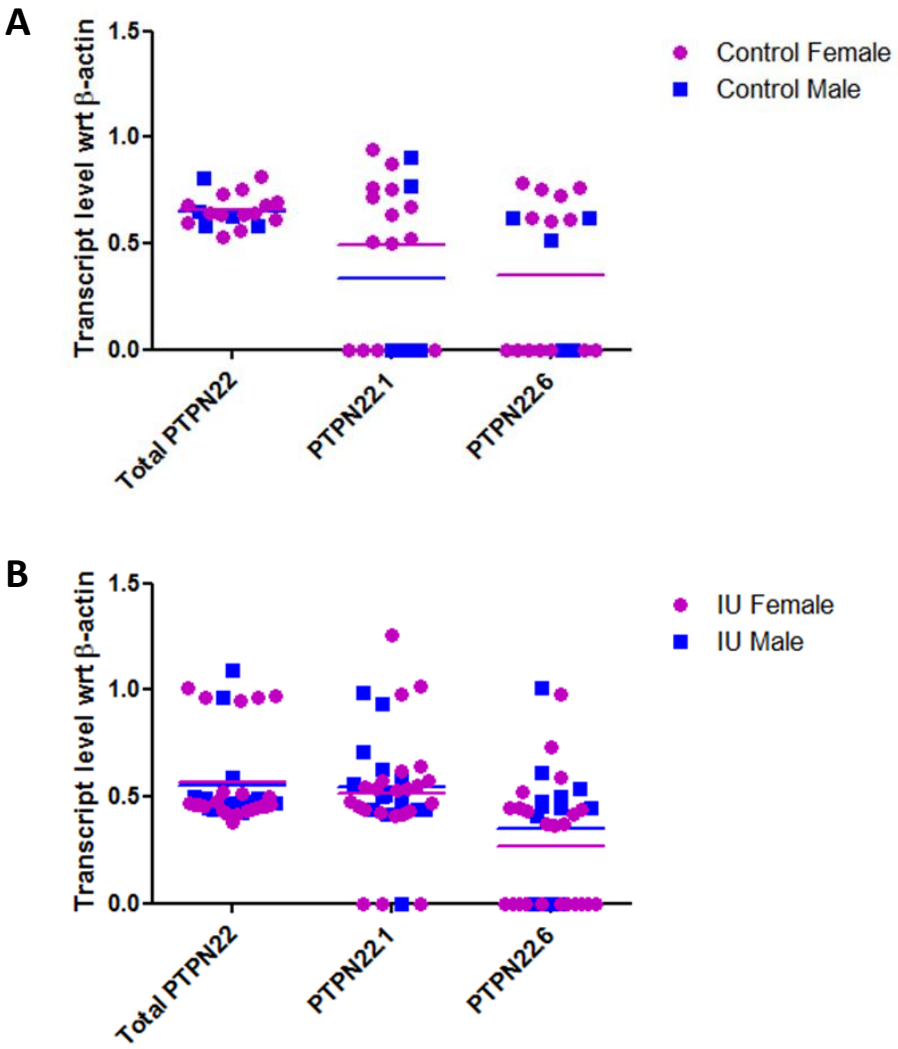

Figure 6|The differences in PTPN22 expression between healthy (a) and IU (b) male and female patients.

4.0 DISCUSSION

4.1 Lyp Expression in Jurkat cells

The Jurkat cell line is a T cell lymphoma cell line that is commonly used to study human T cell function. When jurkat cells were analysed for Lyp protein expression a large number of protein species ranging from 105kDa to 18kDa were detected using a commercially available anti-Lyp antibody. Using the same anti-Lyp antibody, Chang *et al* (2012) uncovered 4 Lyp species within Jurkat cells, all larger than 60kDa, that were not detected in HT-29 cell lysates, a hepatic cancer cell line that does not express PTPN22. Transfection of Jurkat cells with PTPN22 specific siRNA decreased the protein expression of the 4 Lyp protein species, including dominant full-length Lyp, clarifying that these species are either products of Lyp degradation or alternatively spliced isoforms. Chang *et* al (2012) also detected Lyp species smaller than 60kDa, however these were not suppressed by siRNA transfection and are therefore not true Lyp proteins. As PTPN22 siRNAs or negative control cell lines were not available, it is not certain that the smaller unknown Lyp species we detected in jurkat cells are true products of PTPN22 translation.

In the current study full-length Lyp expression increases in Jurkat cells after TCR stimulation. This was anticipated because Lyp associates with many TCR signalling intermediates to negatively regulate T cell activation, and therefore may be induced by TCR stimulation to keep this pathway under control. In addition, the expression of smaller Lyp species increased after stimulation reaching maximal expression on days 5 or 7. It is possible that this is due to increased Lyp turnover leading to more degradation products. However, it could suggest that alternative splicing of Lyp is amplified after stimulation, perhaps as a way to further regulate TCR signalling. It is not known how alternative Lyp isoforms function, therefore they may have complementary roles to full-length Lyp, but also may have contradicting functions in order to help fine tune regulation.

Lyp 2 is an 85kDa Lyp isoform first reported by Cohen *et al* (1999) to be the product of C-terminal alternative splicing. This report found that Lyp 2 could be detected with a rabbit polyclonal antibody against a common C-terminal epitope in resting primary lymphocytes only. After T cell stimulation using either phytohaemagglutinin (PHA) or anti-CD3 Lyp 2 could no longer be detected. Conversely, Chang *et al* (2012) were unable to amplify Lyp 2 from human T cells using Lyp 2 specific primers. The existence of Lyp 2 is therefore debated however differences in the reagents used may account for this. We have shown that a protein species with molecular weight corresponding to Lyp 2 could be detected in resting Jurkat cells and stimulated CD4 T cells taken from IU patients, however its absence from stimulated Jurkat and healthy CD4 T cells is unclear and further questions its existence.

4.2 Lyp Expression in Primary CD4 T cells

An important point of discussion is the dominant expression of smaller Lyp isoforms in CD4 T cells taken from IU patients. Full-length Lyp has until now been known to be the most abundant isoform expressed in primary lymphocytes and cell lines. 3 days after T cell stimulation, Lyp isoforms of 56kDa and 32kDa are clearly found more abundantly in both IU donors (figure 2b) compared to full-length Lyp. This imbalance of Lyp isoforms compared to healthy CD4 T cells may correlate with the presence of IU. Indeed it was found by Ronninger *et al* (2012) that the shorter Lyp isoform Lyp 2 was expressed at significantly lower levels in PBMCs from RA patients compared to healthy controls in a large cohort study. Alternatively, proinflammatory conditions have been suggested to directly alter the PTPN22 transcript profile (Ronninger *et al*, 2012). This could mean that smaller Lyp isoforms are more abundantly produced as a result of pre-existing inflammation caused by IU. Finally, increased expression of smaller Lyp isoforms in donors 1 and 2 may be the result of a PTPN22 SNP resulting in the production of altered Lyp isoforms. We could only be sure

of this by genotyping the donors for common PTPN22 SNPs including the C1858T. As the function of the C1858T Lyp variant is still unknown we can speculate that smaller Lyp isoforms have a loss of phosphatase activity and therefore are less effective at negatively regulating T cell activation, resulting in T cell hyperactivity and predisposition to inflammatory disorders such as IU.

4.3 PTPN22 Gene Expression

SYBR green real-time quantitative PCR was used to assess PTPN22 expression in an attempt to replicate experiments performed by Chang *et al* (2012) in IU patients rather than RA. PTPN22 gene expression stayed at a constant level and did not increase following cell stimulation within Jurkat cells, despite observing an increase in Lyp protein expression. This could be explained by post-transcriptional mRNA regulation by microRNAs, which are small nucleotide sequences that specifically bind to mRNA and prevent its translation into protein. In terms of Lyp, the production or function of microRNAs may be inhibited by cell stimulation allowing maximal protein expression seen as an increase in the western blot. Interestingly, after 1 day of Jurkat cell stimulation PTPN22.6 transcript was detected. It is therefore possible that PTPN22.6 has a role in regulating the translation of full-length Lyp. Chang *et al* (2012) suggests that by altering the level of PTPN22.6 in T cells, PTPN22 activity can be disturbed. In addition, they found that the C1858T SNP enhances phosphatase activity in PTPN22.1 thereby attenuating TCR signalling, but dampens phosphatase activity in PTPN22.6 leading to T cell hyper responsiveness. Therefore the effect of the PTPN22.6/PTPN22.1 ratio on T cell responsiveness to TCR stimulation is likely to influence the balance between self-tolerance and autoimmunity.

A different pattern of PTPN22 gene expression was seen in healthy CD4 T cells. There was an increase in PTPN22 expression following cell stimulation peaking on average by day 3. This could mean that post-transcriptional regulation is not important in primary CD4 T cells suggesting Jurkat

cells may not be an ideal model as once thought. PTPN22.6 transcript was detectable in healthy CD4 T cells as well as IU CD4 T cells providing further evidence for the existence of the splice variant. Interestingly, in donor 3 PTPN22.6 expression reached twice that of donors 1 and 2 on day 7 of cell stimulation. Similarly Chang *et al* (2012) found that out of 3 donors analysed 1 had 60 and 20 times the level of PTPN22.6 expression as the other donors, indicating that variability exists among healthy individuals. It is feasible that these donors expressing a higher amount of PTPN22.6 variant are homozygous for PTPN22.6 as opposed to PTPN22.1 or unknowingly carry a PTPN22 SNP affecting gene splicing. Chang *et al* (2012) found that PTPN22.1 expression was approximately 100 times greater than that of PTPN22.6 in CD4 T cells, whereas in this study PTPN22.6 expression was only marginally less. As identical primers and PCR reagents were used in both studies it is uncertain why this difference occurred.

Analysis of healthy and IU patient DNA samples showed no significant differences in PTPN22 isoform expression between healthy and IU patients, suggesting the presence of the PTPN22.6 splice variant does not correlate with disease as hypothesised. Although after analysing the relationship between PTPN22.1 and PTPN22.6 it was shown that PTPN22.6 homozygotes and .1/.6 heterozygotes were less frequent in the IU cohort of patients. This finding indicates that expression of PTPN22.6 may have a protective effect in IU. Furthermore, multiple PTPN22 SNPs including rs3789607, rs12144309 and rs3811021 have been found to have a protective effect against RA (Taib *et al*, 2010) and PTPN22620W was also found to be protective against Behcet's disease (Baranathan *et al*, 2007). These reports support the possibility of a PTPN22.6 protective effect, however is distinct from that of Chang *et al* (2012), who found a correlation between PTPN22.6 and RA.

There are limitations in our study, notably, in our experiments double-stranded DNA (dsDNA) from patient samples was used to analyse gene expression rather than the single-stranded cDNA analysed previously. As experimental problems were encountered, including absent β-actin expression, a house-keeping gene constitutively expressed in all cells, and highly variable replicate results, using DNA is likely to have affected the accuracy of the protocol. Although the manufacturer's guidelines do mention the use of genomic dsDNA, the PCR conditions used by Chang *et al* (2012) were optimised for cDNA. In addition, SYBR green is a fluorescent dye that non-specifically binds to dsDNA (Ponchel *et al*, 2003). There is likely to be a very high level of non-specific fluorescence emitted if the dsDNA within the patient samples did not completely denature prior to primer annealing or the dye bound to dsDNA prematurely or primer dimers were formed, therefore interfering with accurate gene quantification. A large majority of patient samples did not exhibit the anticipated total PTPN22 expression which was the combined PTPN22.1 and PTPN22.6 transcript level further suggesting a problem with the primer function. Although the primer efficiencies were tested by Chang *et al* (2012) and were all within the recommended efficiency range of 90-110%, we ourselves did not test this which may have consequently affected transcript levels relative to one another. Overall, optimising the SYBR green PCR protocol targeting dsDNA with PTPN22 primers is essential to achieve accurate gene expression quantification and reliable results. Alternative methods of real-time PCR including TaqMan quantitative PCR would give better specificity because the fluorescent reporter probes using in the assay specifically detect a gene of interest rather than all dsDNA.

4.4 Conclusions

This study has provided additional evidence for the existence of the alternatively spliced isoform PTPN22.6 discovered last year. It has also highlighted the potential importance of the balance

between full-length Lyp and PTPN22.6 in IU. The abundance of smaller Lyp isoforms within IU CD4+ T cells, compared to full-length Lyp, suggests an increase in PTPN22.6 could account for pathology and intriguingly Chang *et al* (2012) found an increase in the PTPN22.6/PTPN22.1 ratio to cause T cell hyperresponsiveness. On the contrary, PTPN22.6 homozygotes and PTPN22.1/PTPN22.6 heterozygotes were found more frequently in healthy control patients implying an increase in PTPN22.6 could have a protective effect against IU.

5.0 FUTURE WORK

A different method of real-time PCR to more accurately determine the expression of PTPN22 and PTPN22.6 in T cells from IU and healthy patients is needed. TaqMan qPCR would be a good alternative as it has higher specificity, it's more reproducible and it allows PCR multiplexing, making the detection of multiple PTPN22 splice variants more efficient. cDNA should be obtained from patients T cells for PCRs instead of genomic DNA and genotype IU and healthy patients for known SNPs in PTPN22 including C1858T, rs3789607, rs12144309 and rs3811021 to determine their relationships to the expression of PTPN22 and PTPN22.6.

Detection of PTPN22.6 protein within healthy and IU CD4 T cells using a specific antibody is needed to clarify its presence. CD4 T cell lysates should be analysed by western blotting. Expression of PTPN22.6 protein after TCR stimulation should be investigated to determine its role in T cell activation.

The function of Lyp has been primarily studied in human T cells although Lyp is most abundant in neutrophils. Neutrophils exhibit an overactive phenotype in patients with Behçet's disease, a systemic inflammatory disease that can co-exist with uveitis. Future work would therefore investigate the expression and function of Lyp and its splice variants within neutrophil-like cell lines and primary neutrophils from the peripheral blood of IU and healthy patients. PTPN22 may interact and remove phosphate molecules from substrates within neutrophils. This could be investigated using substrate trapping-mutant PTPs (Flint *et al*, 1997).

6.0 BIBLIOGRAPHY

ARIMUA, Y. & YAGI, J. (2010). Comprehensive Expression Profiles of Genes for Protein Tyrosine Phosphatases in Immune Cells. *Science Signaling*, 3:(137).

ANDERSON, M., VENANZI, E., KLEIN, L., CHEN, Z., BERZINS, S., TURLEY, S., VON BOEHMER, H., BRONSON, R., DIERICH, A., BENOIST, C. & MATHIS, D. (2002). Projection of an Immunological Self Shadow within the Thymus by the Aire Protein. *Science*, 298: 1395-1401.

BABU, BM. & RATHINAM, SR. (2010). Intermediate Uveitis. *Indian Journal of Opthalmology*, 58(1): 21-27.

BARANATHAN, V., STANFORD, M., VAUGHAN, R., KONDEATIS, E., GRAHAM, E., FORTUNE, F., MADANAT, W., KANAWATI, C., GHABRA, M., MURRAY, P. & WALLACE, G. (2007). The Association of the PTPN22 620W Polymorphism with Behcet's Disease. *Annual Rheumatology Disscussion*, 66: 1531–1533.

BEGOVICH, A., CARLTON, V., HONIGBERG, L., SCHRODI, S., CHOKKALINGAM, A., ALEXANDER, H., ARDLIE, K., HUANG, Q., SMITH, A., SPOERKE, J., CONN, M., CHANG, M., CHANG, S.-Y. P., SAIKI, R., CATANESE, J., LEONG, D., GARCIA, V., MCALLISTER, L., JEFFERY, D., LEE, A., BATLIWALLA, F., REMMERS, E., CRISWELL, L., SELDIN, M., KASTNER, D., AMOS, C., SNINSKY, J. & GREGERSEN, P. (2004). A Missense Single-nucleotide Polymorphism in a Gene Encoding a Protein Tyrosine Phosphatase (PTPN22) is Associated with Rheumatoid Arthritis. *American Journal of Human Genetics*, 75: 330-337.

BLANCHETOT, C., CHAGNON, M., DUBE, N., HALLE, M. & TREMBLAY, M. (2005). Substrate-trapping Techniques in the Identification of Cellular PTP Targets. *Methods*, 35: 44–53.

BOTTINI, N., MUSUMECI, L., ALONSO, A., RAHMOUNI, S., NIKA, K., ROSTAMKHANI, M., MACMURRAY, J., MELONI, G., LUCARELLI, P., PELLECCHIA, M., EISENBARTH, G., COMINGS, D. & MUSTELIN, T. (2004a). A Functional Variant of Lymphoid Tyrosine Phosphatase is Associated with Type I Diabetes. *Nature Genetics*, 36: 337-338.

BROWNLIE, RJ., MIOSGE, LA., VASSILAKOS, D., SVENSSON, LM COPE, A. & ZAMOYSKA, R. (2012). Lack of the Phosphatase PTPN22 Increases Adhesion of Murine Regulatory T cells to Improve Their Immunosuppressive Function. *Science Signaling*, 5(252).

BURN, G., SVENSSON, L., SANCHEZ-BLANCO, C., SAINI, M. & COPE, A. (2011). Why is PTPN22 a Good Candidate Susceptibility Gene for Autoimmune Disease? *FEBS letters*, 585: 3689-3698.

CARLTON, V., HU, X., CHOKKALINGAM, A., SCHRODI, S., BRANDON, R., ALEXANDER, H., CHANG, M., CATANESE, J., LEONG, D., ARDLIE, K., KASTNER, D., SELDIN, M., CRISWELL, L., GREGERSEN, P., BEASLEY, E., THOMSON, G., AMOS, C. & BEGOVICH, A. (2005). PTPN22 Genetic Variation: Evidence

for Multiple Variants Associated with Rheumatoid Arthritis. *American Journal of Human Genetics*, 77: 567-581.

CASPI, R. (2010). A Look at Autoimmunity and Inflammation in the Eye. *Journal of Clinical Investigation,* 120(9): 3073–3083.

CHANG, JH., MCCLUSKEY, PJ. & WAKEFIELD, D. (2005). Acute Anterior Uveitis and HLA-B27. *Survey of Ophthalmology*, (4): 364-88.

CHANG, H.-H., TAI, T.-S., LU, B., IANNACCONE, C., CERNADAS, M., WEINBLATT, M., SHADICK, N., MIAW, S.-C. & HO, I. C. (2012). PTPN22.6, a Dominant Negative Isoform of PTPN22 and Potential Biomarker of Rheumatoid Arthritis. *PloS One*, 7(3): 1-7.

CHIEN, W., TIDOW, N., WILLIAMSON, E., SHIH, L., KRUG, U., KETTENBACH, A., FERMIN, A., ROIFMAN, C. and KOEFFLER, H. (2003). Characterization of a Myeloid Tyrosine Phosphatase, Lyp, and Its Role in the Bcr-Abl Signal Transduction Pathway. *The Journal of Biological Chemistry,* 278: 27413-27420.

COHEN, S., DADI, H., SHAOUL, E., SHARFE, N. & ROIFMAN, C. (1999). Cloning and Characterization of a Lymphoid-specific, Inducible Human Protein Tyrosine Phosphatase, Lyp. *Blood*, 93: 2013-2024.

EKSIOGLU-DEMIRALP, E., DIRESKENELI, H., KIBAROGLU, A. & YAVUZ, S. (2001). Neutrophil Activation in Behcet's Disease. *Clinical and Experimental Rheumatology*, 19 (Suppl. 24): S19-S24.

FLINT, A., TIGANIS, T., BARFORD, D. & TONKS, N. (1997). Development of "Substrate-trapping" Mutants to Identify Physiological Substrates of Protein Tyrosine Phosphatases. *Proceedings of the National Academy of Sciences of the United States of America*, 94: 1680-1685.

GOODNOW, C. (2007). Multistep Pathogenesis of Autoimmune Disease. *Cell*, 130: 25-35.

GREGERSEN, P., LEE, H.-S., BATLIWALLA, F. & BEGOVICH, A. (2006). PTPN22: Setting Thresholds for Autoimmunity. *Seminars in Immunology*, 18: 214-223.

JANEWAYS, C. (2008). Janeway's Immunobiology. Seventh Edition. Abingdon: Garland Science, Taylor & Francis Group.

LOPEZ-ESCAMEZ, JA. (2010). A Variant of PTPN22 Gene Conferring Risk to Autoimmune Diseases May Protect Against Tuberculosis. *Journal of Postgraduate Medicine*, 56(3): 242-3.

KAWASAKI, E., AWATA, T., IKEGAMI, H., KOBAYASHI, T., MARUYAMA, T., NAKANISHI, K., SHIMADA, A., UGA, M., UGA, M., KURIHARA, S., KAWABATA, Y., TANAKA, S., KANAZAWA, Y., LEE, I. & EGUCHI, K. (2006a). Systematic Search for Single Nucleotide Polymorphisms in a Lymphoid Tyrosine Phosphatase Gene (PTPN22): Association Between a Promoter Polymorphism and Type 1 Diabetes in Asian Populations. *American Journal of Medical Genetics*. Part A, 140: 586-593.

KUO, N., LYMPANY, PA., MENEZO, V., LAGAN, AL., JOHN, S., YEO, TK., LIYANAGE, S., DU BOIS, RM., WELSH, K. & LIGHTMAN, S. (2005). TNF−857T, a Genetic Risk Marker for Acute Anterior Uveitis. *Investigation of Ophthalmology Vision Science*, 46(5): 1565-1571.

MARTIN, TM., BYE, L., MODI, N., STANFORD, MR., VAUGHAN, R., SMITH, JR., WADE, NK., MACKENSEN, F., SUHLER, EB., ROSENBAUM. JT. & WALLACE, GR. (2009). Genotype Analysis of Polymorphisms in Autoimmune Susceptibility Genes, CTLA-4 and PTPN22, in an Acute Anterior Uveitis Cohort. *Molecular Vision*, 15: 208-12.

MATTAPALLIL, M., SAHIN, A., SILVER, PB., SUN, S., CHAN, C., REMMERS, EF., HEJTMANCIK, JF., CASPI, R. (2008). Common Genetic Determinants of Uveitis Shared with Other Autoimmune Disorders. *The Journal of Immunology*, 180(10): 6751-6759.

PONCHEL, F., TOOMES, C., BRANSFIELD, K., LEONG, F., DOUGLAS, S., FIELD, S., BELL, S., COMBARET, V., PUISIEUX, A., MICHELL, A., ROBINSON, P., INGLEHEARN, C., ISSACS, J. & MARKHAM, A. (2003). Real-time PCR Based on SYBR-Green I Fluorescence: An Alternative to the TaqMan Assay for a Relative Quantification of Gene Rearrangements, Gene Amplifications and Micro Gene Deletions. *BMC Biotechnology*, 3: 18.

READ, RW. (2006). Uveitis: Advances in Understanding of Pathogenesis and Treatment. *Current Rheumatology Reports*, 8: 260–266.

READ, RW., SZALAI, AJ., VOGT, SD., MCGWIN, G. & BARNUM, SR. (2006). Genetic Deficiency of C3 as well as CNS-targeted Expression of the Complement Inhibitor sCrry Ameliorates Experimental Autoimmune Uveoretinitis. *Experimental Eye Research*, 82(3): 389-94.

RIECK, M., ARECHIGA, A., ONENGUT-GUMUSCU, S., GREENBAUM, C., CONCANNON, P. & BUCKNER, J. (2007). Genetic Variation in PTPN22 Corresponds to Altered Function of T and B Lymphocytes. *Journal of Immunology*, 179: 4704-4710.

RONNINGER, M., GUO, Y., SHCHETYNSKY, K., HILL, A., KHADEMI, M., OLSSON, T., REDDY, P., SEDDIGHZADEH, M., CLARK, J., LIN, L.-L., O'TOOLE, M. & PADYUKOV, L. (2012). The Balance of Expression of PTPN22 Splice Forms is Significantly Different in Rheumatoid Arthritis Patients Compared with Controls. *Genome Medicine*, 4: 2.

SMITH-GARVIN, J., KORETZKY, G. & JORDAN, M. (2009). T Cell Activation. *Annual Review of Immunology*, 27: 591-619.

STANFORD, S., MUSTELIN, T. & BOTTINI, N. (2010). Lymphoid Tyrosine Phosphatase and Autoimmunity: Human Genetics Rediscovers Tyrosine Phosphatases. *Seminars in Immunopathology*, 32: 127-136.

TAIB, W., SMYTH, D., MERRIMAN, M., DALBETH, N., GOW, P., HARRISON, A., HIGHTON, J., JONES, P., STAMP, L., STEER, S., TODD, J. & MERRIMAN, T. (2010). The PTPN22 Locus and Rheumatoid

Arthritis: No Evidence for an Effect on Risk Independent of Arg620Trp. *PLoS ONE*, 5(10): e13544. doi:10.1371/journal.pone.0013544.

TAUTZ, L. (2012). PTPhome-PTPN22. [online]. Available at: http://www.ptphome.net/resourcemolpages/ ptpn22.html. [Accessed on 1 May 2013].

VANG, T., CONGIA, M., MACIS, M., MUSUMECI, L., ORR, V., ZAVATTARI, P., NIKA, K., TAUTZ, L., TASKN, K., CUCCA, F., MUSTELIN, T. & BOTTINI, N. (2005). Autoimmune-associated Lymphoid Tyrosine Phosphatase is a Gain-of-function Variant. *Nature Genetics*, 37: 1317-1319.

VERITY, DH., WALLACE, GR., VAUGHAN, RW., STANFORD, RW., (2003). Behçet's Disease: from Hippocrates to the Third Millennium. *British Journal of Ophthalmology*, 87: 1175-1183.

WAKEFIELD, D., BUCKLEY, R., GOLDING, J., MCCLUSKEY, P., ABI-HANNA, D., CHARLESWORTH, J. & PUSSELLA, B. (1988). Association of Complement Allotype C4B2 with Anterior Uveitis. *Human Immunology*, 21: 233-237.

WANG, S., DONG, H., HAN, J., HO, W., FU, X. & ZHAO, Z. (2010). Identification of a Variant Form of Tyrosine Phosphatase LYP. *BMC Molecular Biology*, 11: 78.

ZHANG, J., ZAHIR, N., JIANG, Q., MILIOTIS, H., HEYRAUD, S., MENG, X., DONG, B., XIE, G., QUI, F., HAO, Z., MCCULLOCH, CA., KEYSTONE, EC., PETERSON, AC. & SIMINOVITCH, KA. (2011). The Autoimmune Disease-associated PTPN22 Variant Promotes Calpain-mediated Lyp/Pep Degradation Associated with Lymphocyte and Dendritic Cell Hyperresponsiveness. *Nature Genetics*, 43(9): 902-7.

ZHENG, P. & KISSLER, S. (2012). PTPN22 Silencing in the NOD Model Indicates the Type 1 Diabetes-associated Allele is Not a Loss-of-function Variant. *Diabetes*, 62(3): 896-904.

Abstract

BACKGROUND:

Adoptive T cell therapy (ACT) for cancer involves the *ex vivo* expansion and infusion of tumour-specific T cells. T cell specificity can be genetically engineered using chimeric antigen receptor (CAR) gene transfer. A CAR combines MHC-independent antibody recognition with downstream T cell signalling and cytotoxicity. Less differentiated T cells are more suitable for ACT because they show enhanced persistence and anti-tumour activity *in vivo* compared to effector T cells. Cord blood mononuclear cells (CBMCs) are dominated by naïve T cells, therefore are a potential source for CAR ACT.

METHODS:

Peripheral blood mononuclear cells (PBMCs) (n=7) and CBMCs (n=9) were retrovirally transduced with a CAR targeting a tumour vasculature antigen. Cells were analysed for the differentiation markers CCR7 and CD45R using flow cytometry before and after transduction, and the IFNγ response to target antigen was assessed by ELISAs.

RESULTS:

CBMCs achieved transduction rates indistinguishable to that of PBMCs but retained a significantly less differentiated phenotype after CAR transduction in CD4 and CD8 subsets. Some transduced CBMC donors produced significantly less IFNγ in response to target antigen while others produced none.

CONCLUSIONS:

CBMCs are an attractive alternative source for CAR ACT.

Table of Contents

1.0 INTRODUCTION

1.1 Cancer

The regulation of the cell cycle is essential in keeping cell growth and number in check. Key players in this regulation are cyclin proteins and cyclin-dependent kinases (CDKs) which associate with one another at appropriate times during the cell cycle to allow progression of cell division. Mutations within proteins that regulate the cell cycle can result in rapid and out of control cell division leading to tumour formation; this is termed cancer [1]. Tumours can invade and destroy surrounding tissues leading to organ failure and death, therefore the removal of cancerous cells is vital.

1.12 Graft-Versus-Leukaemia and Adoptive T cell Therapy

Life-threatening cancers can be treated with haematopoietic stem cell transplantation (HSCT), in which haematopoietic stem cells (HSCs) isolated from either the patient themselves: an autologous transplant, or a human leukocyte antigen (HLA)-matched donor: an allogeneic transplant, are adoptively transferred [2][3]. A major complication of allogeneic HSCTs is graft-versus-host disease (GVHD), in which donor lymphocytes present within the transplant recognise and attack self-antigens in the recipient leading to severe inflammation. Although GVHD is a large limitation of HSCTs, reciprocally there is also evidence of a graft-versus-leukaemia (GVL) phenomenon, in which donor lymphocytes within the transplant attack malignant cells causing tumour regression [4][5]. Identification of this anti-tumour adoptive therapy has driven the development of targeted immunotherapies to treat cancer. For example, adoptive T-cell therapy (ACT) can be utilised where donor lymphocytes naturally expressing T-cell receptors (TCRs) specific for tumour-associated antigens (TAAs) can be isolated and expanded *in vitro* before being

adoptively transferred into a patient to induce an immune response against a specific TAA and hopefully avoid GVHD [5].

1.13 Adoptive Therapy with Tumour-Infiltrating Lymphocytes

The histological analysis of tumours has revealed populations of tumour-infiltrating lymphocytes (TILs) [6]. The Rosenberg group at the National Cancer Institute suggested that TILs remain in the tumour microenvironment because they recognise TAAs and have specific cytolytic activities [7]. Since this finding, ACT using autologous TILs has become a realistic adoptive immunotherapy. The *ex vivo* techniques used to create TIL adoptive therapies are outlined in figure 1 [8]. Giving lymphodepleting therapy prior to ACT has been shown to markedly improve antitumour efficacy, probably due to the elimination of immunosuppressive regulatory T cells and competition for cytokines and APCs from other lymphocytes [9]. Although ACT using TILs has been successful in causing tumour regression in melanoma patients [10], strong evidence for this in other common cancers such as breast, prostate and ovarian has not been shown [11]. In addition, the lack of potent TILs and the length of time needed to generate a sufficient number are not ideal in the clinical setting. To circumvent these limitations, new strategies to genetically modify the specificity of T cells to target certain TAAs have been developed.

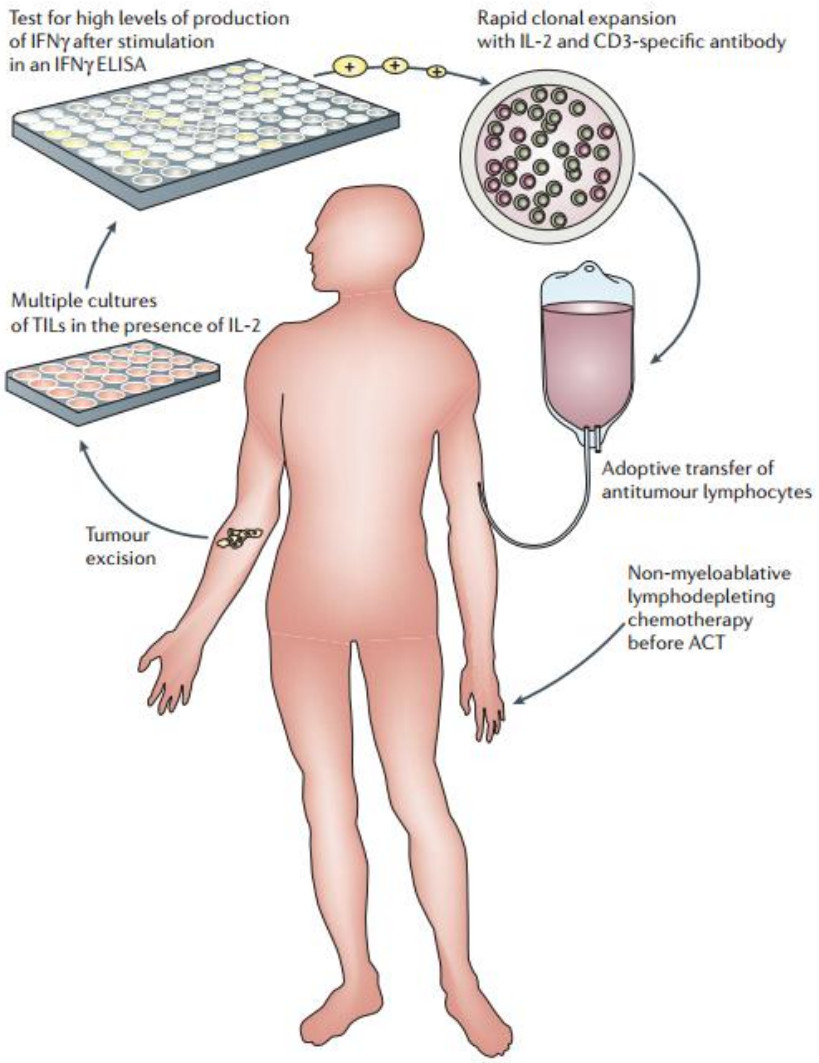

Figure 1|Generating autologous adoptive immunotherapy using tumour- infiltrating lymphocytes [8]. Where possible, tumour biopsies are a valuable source of TILs. TILs are extracted from tumour biopsies and cultured in the presence of a high concentration of IL-2. Tumour-specific TILs are selected by culturing them with autologous or allogeneic HLA-matched tumour-cell lines and assaying for the secretion of IFN-γ. Potent tumour-specific lymphocytes are then expanded rapidly *in vitro* using exogenous IL-2, anti-CD3 antibodies and irradiated peripheral blood mononuclear cells (PBMCs) as feeder cells. Patients are then given non-myeloablative lymphodepleting chemotherapy before the expanded tumour-specific lymphocytes are adoptively transferred via intravenous injection.

1.2 TCR-Modified T Cells

1.21 T Cell Recognition and TCR Signalling

The genetic engineering of T cells has dramatically advanced the field of immunotherapy and provided potential for not only cancer therapy but also for treating viral infections such as EBV. Every T cell expresses its own TCR with unique peptide specificity, created by somatic rearrangement of TCR gene segments during T cell development. When a T cell encounters its cognate antigen, in the context of HLA molecules, the TCR propagates downstream signalling resulting in T cell activation. Complete T cell activation requires two signals: signal 1 provided by TCR/HLA recognition and signal 2 provided by costimulation. CD28 is one such costimulatory molecule expressed on the surface of T cells and upon ligation with its ligands, CD80 and CD86 present on APCs, it mediates costimulatory signals to the T cell and permits full T cell activation [12]. The resulting T cell is capable of target cell lysis, via cytotoxic mediators such as perforin, and cytokine secretion (e.g. interleukin-2) and in this way may be capable of mediating anti-tumour effects.

1.22 Tumour-reactive TCR Gene Transfer

Naturally occurring tumour specific T cells are rare and frequently undetectable in most patients. To overcome this problem, genetically-modified donor T cells re-directed against TAAs have been engineered [13]. TCR α and β chain genes can be inserted into gene transfer vectors, commonly retro- or lenti- viral vectors, that will facilitate the stable integration of TCR genes into donor T cell genomes. If successful, the resulting T cell will express this “exogenous” TCR and confer upon the engineered cell the same antigenic specificity as the original T cell from which the TCR was cloned. If required, the engineered T cells can then be expanded into large quantities *in vitro* [11].

During genetically modified TCR gene rearrangement in mice, there is evidence of mismatch pairing between exogenous α and β TCR chains and pre-existing endogenous α and β chains in mice [14]. This presents a risk for self-antigen recognition leading to autoimmunity, and is a threat that needs consideration. In addition, there is a risk of insertional mutagenesis during transduction of TCR receptor genes that may activate oncogenes or switch off tumour suppressor genes and induce T cell lymphomas. These factors make TCR gene transfer potentially unsafe in the clinic, however it is suggested that the insertion of additional disulphide bonds between exogenous α and β chains can prevent their mispairing [15]. Some TCR transfer-based therapies have been successful in treating cancers such as targeting MART1 in metastatic melanoma [16], but the availability of this treatment is partly limited due to the requirement for HLA matching (i.e. the patient has to carry the restricting HLA allele for the TCR being transferred).

1.3 Chimeric Antigen Receptors

Redirecting the specificity and function of T cells using a chimeric antigen receptor (CAR) was first performed by Gross *et al* [17], which brought together the idea of combining B cell receptor (BCR) antibody recognition with TCR signalling. A CAR is most commonly composed of a single chain variable fragment (scFv) that is derived from the heavy and light variable chain sequences of an antibody recognising a molecule of interest (Figure 2). The scFv chains are linked together and fused to a CD3ζ transmembrane chain by a flexible hinge region which converts antibody:antigen recognition into downstream signalling, allowing T cell activation and targeted cytolytic activity. The earliest CARs containing only a scFv and CD3ζ domain are termed “first generation CARs” and although they can mediate targeted destruction of cancers in vitro and in mouse models they have shown poor efficacy in clinical trials.

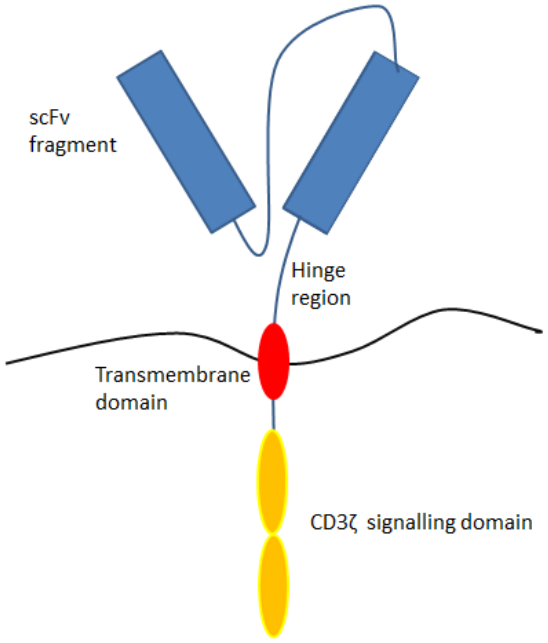

Figure 2|Schematic of a First Generation Chimeric Antigen Receptor. A first generation CAR commonly contains a scFv region derived from the heavy and light chain variable regions of an antibody with specificity of interest. The scFv is attached to a hinge region which inserts into the cell surface and is fused to the CD3ζ signalling domain allowing T cell signalling following CAR engagement.

1.31 CAR Signalling

A major advantage of CAR gene transfer compared to TCR gene transfer is that CARs recognise 3D structures and is therefore HLA-independent. This means that CAR-modified T cells can be infused into patients regardless of their HLA type, and so is much more beneficial in treating a broader range of patients. Furthermore, this renders tumour cells unable to avoid immune detection by down regulating HLA class I molecules.

Unlike TCR signalling, CAR signalling is not physiological and therefore may involve slightly different mechanisms. In an attempt to replicate TCR signalling, second and third generation CARs were developed, which include the addition of either one, or more than one costimulatory domains respectively. Some costimulatory domains that have been utilised within CAR constructs are CD28, 4-1BB, OX40, or CD27 [18]. The addition of costimulatory domains has provided more robust T cell activation and functionality in a number of experimental settings. CD19-specific CARs carrying the CD28 costimulatory domain provided more potent anti-tumour activity against $CD19^{+}$ B cells and greater T cell persistence when adoptively transferred *in vivo* [19]. Furthermore, CD19-

specific CAR constructs carrying the 4-1BB costimulatory domains were also successful in treating three patients with chronic lymphocytic leukaemia (CLL) [20]. Second generation CARs targeting prostate membrane-specific antigen (PSMA) containing a CD28 signalling domain showed greater IL-2 secretion, enhanced proliferation and PSMA target cell lysis [21]. Third generation CARs were expected to mediate even more potent anti-tumour properties due to enhanced costimulation. Although this was seen in some experimental settings [22, 23], Wilkie *et al* (2008) found no difference in *in* vitro cytotoxicity between second and third generation CAR transduced cells targeting MUC1 [24]. Consequently it remains unclear which CAR design is most optimal and is likely to depend on the scFv design, the target antigen, the method of CAR transduction and type of host cell transduced, the *in vivo* tumour model used and the culture method used.

In addition, delivering proinflammatory cytokines such as IL-12, IL-7, IL-15 and IL-21 to the local tumour environment in combination with CAR targeting to enhance anti-tumour activity has been investigated [25]. IL-12 is a potent proinflammatory cytokine that has been shown to enhance CAR-transduced $CD8^+$ T cell functionality. Although these cells did not persist long *in vivo* large numbers of cells were found intratumourally, suggesting the delivery of IL-12 could enable fewer T cells to be administered to achieve tumour regression [26].

1.32 CAR Target Design

Utilising CAR technology has both advantages and disadvantages in antigen targeting. The antibody nature of a CAR means they can only recognise antigens expressed on the cell surface, as intracellular antigens must be processed and presented in a different manner via HLA. The benefit of CARs is that they can recognise not only peptides, but also carbohydrates and glycolipids providing a much broader range of potential therapeutic targets. The key to successful CAR therapy is in choosing a target that is specifically expressed at a higher concentration on tumour

cells and compared to the rest of the body, to prevent the risk of 'on-target off-tissue toxicity' in which CAR-modified T cells attack non- cancerous cells. One such target already being explored is CD19 for the treatment of $CD19^+$ B cell leukemias. CD19 is a surface antigen expressed on normal and leukemic B cells but not HSCs; therefore targeting this molecule will eradicate malignant B cells and the normal B cell pool whilst sparing B cell precursors. The first successful case of anti-CD19 CAR immunotherapy was published by Rosenberg and co-workers at the National Cancer Institute [27]. Although many successes using CD19-specific T cells have been reported, it is also important to note that adverse effects and mortalities using TCR and CAR transfer have been reported. Most recently, the severe on-target off-tissue toxicity of an anti-melanoma-associated Ag A3 (MAGE) TCR gene therapy was reported, in which two patients developed necrotizing leukoencephalopathy resulting in their death [28]. In addition, a transient but severe colitis was induced in all metastatic colorectal cancer patients treated with T cells targeting carcinoembryonic antigen (CEA), although one patient did have regression of metastases in the liver and lung [29]. Finally, a patient who received CAR therapy targeting ERBB2, a receptor overexpressed in 15-25% of breast cancers, experienced respiratory distress within 15 minutes of intravenously receiving 10^{10} cells. The patient died 5 days later likely due to a large cytokine storm in the lungs caused by low level expression of ERBB2 on lung epithelium [30]. Cases like this highlight the importance for selecting an immunotherapy target that is specific to malignant cells and rigorous preclinical testing *in vitro* and in animal models.

Following numerous severe adverse events in clinical trials safety precautions including the addition of suicide genes have been considered. Caspase-9 is an enzyme that induces apoptosis and has been successfully incorporated into genetically modified T cells to act as a safety switch if therapy becomes toxic. The administration of a prodrug switched on the production of caspase-9,

activating the apoptotic pathway and eliminating 90% of circulating transferred cells within 30 minutes [31]. Other safety strategies include transfecting T cells with CAR RNA so that CAR expression is only transient, and controlling CAR expression via an incorporated regulatory gene that can be switched on or off after administration of a small molecule [18].

1.33 Tumour Vasculature

Tumour endothelial markers (TEMs) are molecules identified within the tumour endothelial vasculature that are not present or present at very low concentrations on normal vasculature and therefore hold obvious therapeutic potential. In the adult, the production of new blood vessels, termed angiogenesis, is induced by local hypoxia which consequently induces the expression of vascular endothelial growth factors (VEGFs) and the growth of endothelium. When a tumour exceeds $2mm^3$ in volume it becomes hypoxic, thus inducing local angiogenesis to facilitate tumour growth in a crucial checkpoint called the angiogenic switch. Tumour vasculature is structurally and functionally abnormal from that of normal tissue. Blood vessels within tumours have varying diameters and are disorganised, thin, and leaky, making tumour blood perfusion poor [32]. These morphological differences are advantageous in finding molecular differences between normal and tumour vascular endothelium. As tumours require a blood supply to survive, targeting the tumour vasculature with immunotherapy in an attempt to destroy its blood supply could cause regression in all solid tumours.

1.34 CLEC14A

The novel TEM CLEC14A has recently been discovered by Bicknell *et al* through bioinformatics data mining [33]. CLEC14A is a member of the type 14 calcium dependent C-type lectins and is expressed on vasculature endothelium. siRNA knock-down experiments of CLEC14A have uncovered its role in endothelial cell-cell adhesion and angiogenesis [34]. Double immunostaining

of healthy and carcinoma tissue arrays for CLEC14A and the endothelial marker Ulex lectin, revealed strong expression of CLEC14A on vasculature endothelium on a wide range of cancer types compared to very low or no expression on healthy tissue (Figure 3). Using micro array analysis of gene expression, CLEC14A was also shown to be up-regulated on human umbilical vein endothelial cells (HUVEC) when under low shear stress conditions (i.e. grown in static culture). As tumour blood perfusion is known to be poor, the strong staining of CLEC14A seen within tumour vasculature correlates with this finding of expression on endothelial cells exposed to low shear stress [33].

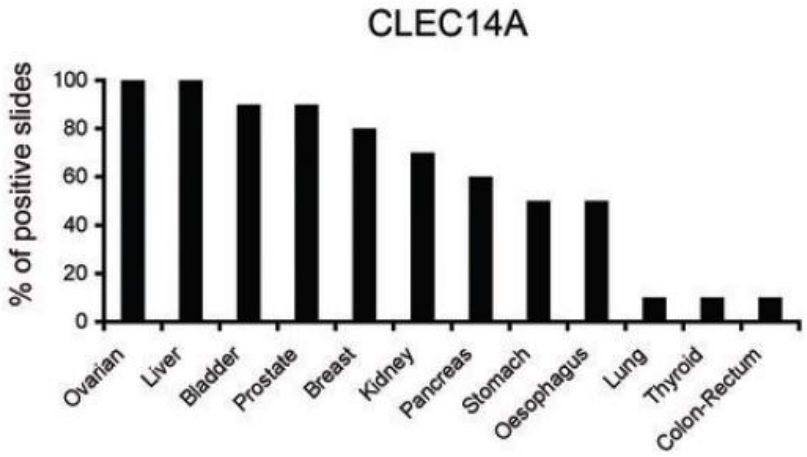

Figure 3 | CLEC14A Expression in Multiple Cancer Tissue Samples. Double immunostaining for CLEC14A and Utex lectin shows between 50 and 100 percentage positive staining in all cancer types analysed except lung, thyroid and colon-rectum cancer [33].

1.4 CAR Host Cells

1.41 T Cell Subsets for ACT

There is great controversy over which is the best T cell subset for targeted ACT. The ideal would be a T cell that is capable of expanding and persisting long-term, entering peripheral tissues, recognising tumour antigen specifically and mounting a cytolytic response. T cells are a heterogeneous population of cells that can be divided into functionally distinct subsets based on the expression of cell surface markers including CC-chemokine receptor 7 (CCR7) and CD45RA.

Naïve T cells (T_N) that have not yet recognised antigen are positive for both CCR7 and CD45RA allowing them to traffic through secondary lymphoid organs and interact with antigen presenting cells. As T cells encounter antigen they differentiate into central memory (Tcm) and effector memory (Tem) T cells that begin to express a different CD45 isotype, CD45RO. Effector T cells also down regulate CCR7 and acquire cytokine effector functions. Tcm cells continue to express CCR7 enabling these cells to recirculate to lymphoid organs [35]. Most recently a memory stem-cell like population has been identified (Tscm) displaying a $CCR7^+$ $CD45RA^+$ naive phenotype but also expressing high levels of CD95, IL-2Rb, CXCR3, and LFA-1 [36]. The antitumour properties of different T cell subsets have been compared and have shown Tem cells to have the least antitumour potency, followed by Tcm and finally Tn and Tscm cells [37]. It would be reasonable to expect Tem cells to be the most effective subset for ACT due to their effector functions; however reports have shown that less-differentiated T cells have increased antitumour efficacy *in vivo* [38]. There are a number of reasons why this might be including their ability to proliferate and expand, persist for a sufficient length of time and migrate to sights of malignancy *in vivo*. Paradoxically, more differentiated $CD8^+$ Tem cells showed increased antitumour properties *in vitro* but when infused into tumour-bearing mice their efficacy was poor compared to more naïve T cell phenotypes largely because the more differentiated cells failed to expand and persist following infusion [39, 40]. This presents a challenge for researchers developing antitumour immunotherapies and may suggest that *in vivo* experiments should be carried out earlier to fine tune therapies.

1.42 Human Umbilical Cord Blood T Cells

Human umbilical cord blood (HUCB) taken from the mother during child birth is a valuable source of haematopoietic cells. It has been found that around 90% of cord blood mononuclear cells

(CBMCs) found within HUCB express the immature phenotypic marker CD45RA compared to around 50% of T cells in adult peripheral blood [41]. Freshly isolated CBMCs were also functionally immature and produced no cytotoxicity when analysed by lectin-dependent cell-mediated cytotoxicity assays (LDCC) in the presence of phytohemagglutinin (PHA) [41]. Upon stimulation, CBMCs produced minimal responses in mixed lymphocyte reactions and cytolytic assays, produced no effector cytokines, and contained fewer cytolytic $CD8^+$ T cells, giving evidence that CBMCs have poor functional activity *in vitro* [41]. Many reports have shown CBMC immaturity since these findings [42] and it is hypothesised that this is why HUCB transplants are well tolerated and carry a decreased risk of GVHD, compared to MHC-matched allogeneic bone marrow transplants [43]. One possibility suggested in the literature is a deficiency in CD3/CD28 signalling in CBMCs, resulting is dysregulated Fas-L-mediated cell cytotoxicity [44]. Their use is therefore also of interest for immunotherapy, as less differentiated T cells are shown to be more efficacious in ACT. In 1983 the transformation of CBMCc with a human T-cell lymphoma virus was first achieved, and has subsequently directed the viral vector transfer of TCR and CAR genes into CBMCs [45]. Recently, CBMCs have been transduced to express a TCR specific for and EBV protein LMP2 and these cells were shown to function in an antigen-specific manner, but importantly they displayed a less differentiated phenotype than adult T cells engineered in the same manner [46]. Given the therapeutic possibilities of CARs, this project was designed to explore the possibility of engineering CBMCs to express CARs and then to explore their function and differentiation status to determine if they may be a more appropriate host cell for CAR-based therapies.

1.5 Aims

1. To successfully retrovirally transduce PBMCs and CBMCs with a CRT3-second generation CAR recognising CLEC14A.

2. To analyse and compare the differentiation status of resting and transduced PBMCs and CBMCs using cell-surface fluorescent antibody staining and flow cytometry.
3. To assess and compare the *in vitro* anti-tumour function of transduced PBMCs and CBMCs using IFNγ ELISAs.

1.6 Hypothesis

I hypothesise that resting CBMCs will contain a greater percentage of $CCR7^+$ $CD45RA^+$ Tn cells compared to PBMCs. Following CAR transduction I predict both CBMCs and PBMCs will differentiate, however CBMCs will retain an earlier differentiation phenotype than PBMCs. I therefore also predict that transduced CBMCs will exhibit some anti-tumour functions but will not be as potent as PBMCs, as PBMCs will consist of more differentiated effector T cells which carry anti-tumour functions.

2.0 Materials and Methods

2.1 List of Reagents and Media

Reagent or Media	Ingredients
Complete RPMI	RPMI (Roswell Park Memorial Institute) 1640 [Sigma-Aldrich, Gillingham, UK], 1% GPS (2mM L-glutamine [Gibco], 100U/ml penicillin [Sigma], 100µg/ml streptomycin [Sigma]) 10% Fetal Bovine Serum (FBS) [Biosera, Ringmer, UK]
Phosphate Buffer Saline (PBS)	PBS tablet [Oxoid, Basingstoke, UK] dissolved in 100mls of distilled water
Freezing Media	90% FBS [Biosera, Ringmer, UK], 10% Dimethyl Sulfoxide (DMSO) [Fisher Scientific, Loughborough, UK]
T cell media (TCM)	Complete RPMI containing 1% Human Serum [Biosera, Ringmer, UK]
Complete (Dulbecco's Modified Eagle Medium) DMEM	DMEM [Sigma-Aldrich, Gillingham, UK], 10% FBS [Biosera, Ringmer, UK] 1% GPS (2mM L-glutamine, 100U/ml penicillin, 100µg/ml streptomycin)
Transfection Media	DMEM [Sigma-Aldrich, 10% FBS [Biosera, Ringmer, UK], 2mM L-glutamine
MACs buffer	PBS, 2mM ethylenediamine tetra-acetric acid (EDTA) [Sigma-Aldrich, Gillingham, UK], 0.5% BSA [Sigma-Aldrich, Gillingham, UK]
ELISA Media	TCM supplemented with 25IU/ml IL-2 [Novartis, UK]
Coating buffer	0.1M Na2HPO4 adjusted to pH9 with 0.1M NaH2PO4
Blocking Buffer	1% (w/v)Bovine serum albumin [Sigma-Aldrich, Gillingham, UK] in PBS (filtered 0.45um) with 0.05% (v/v) Tween-20 (50µl/100ml) [Sigma-Aldrich, Gillingham, UK]

2.2 Cell Culture and Isolation

2.21 Peripheral Blood Mononuclear Cells (PBMCs) Isolation and Stimulation

Healthy PBMCs were isolated from leukoreduction system chambers kindly provided by the National Blood Service using the lymphoprep [Axis-Shield, Dundee, UK] gradient centrifugation technique. The ~10ml cell suspension obtained from the chamber was diluted 1:5 in warm complete RPMI and gently layered onto lymphoprep. Blood was then centrifuged at 800g for 30 minutes at room temperature with no braking. The PBMC layer was harvested and washed three times in complete RPMI before cells were counted using a haemocytometer and resuspended at $100x10^6$/ml in freezing media and cryopreserved. When needed, PBMCs were thawed at 37°C immediately before being washed twice in warm TCM and spun at 400g for 5 minutes. PBMCs were resuspended at a concentration of $1x10^6$ in T cell media TCM containing OKT3 (30ng/ml) [Janssen Cilag, UK] and IL-2 (300IU/ml) [Novartis, UK] and cultured for 48 hours at 37°C, 5% CO_2 prior to CAR transduction.

2.22 Cord Blood Mononuclear Cells (CBMC) Preparation and Stimulation

HUCB transfusion bags that were not suitable for patient transplant were kindly provided by the National Blood Service. CBMCs were isolated from HUCB via lymphoprep density centrifugation and cryopreserved. When needed, CBMCs were thawed at 37°C immediately before being diluted slowly in cold complete RPMI and left to rest for 15 minutes. Cells were then washed twice at 400g for 5 minutes in warm complete RPMI and counted using a haemocytometer. Cells were resuspended at a concentration of $1x10^6$/ml in TCM containing OKT3 (30ng/ml) and IL-2 (300IU/ml) and cultured for 48 hours at 37°C, 5% CO_2 prior to CAR transduction. PBMC and CBMC donors provided written consent for their blood to be used for research. Ethical approval for this

study was provided by the Birmingham East, North and Solihull Research Ethics Committee (Ref 05/Q2706/91).

2.23 Indiana Phoenix A Cell Culture

A viral packaging cell line, Phoenix A cells, from the Nolan lab at Stanford University were cultured in complete DMEM in T75 flasks [Sarsteadt, Leicester, UK]. Phoenix cells were washed with 10mls of sterile PBS and trypsinised with 1X trypsin-EDTA [Gibco, UK] to a single cell suspension. The trypsin was inactivated with addition of transfection media, counted using a haemocytometer and spun at 400g for 3 minutes. $2x10^6$ or $6x10^6$ Phoenix A cells were resuspended in 10mls or 25mls of transfection media and cultured overnight in a T25 or T75 flasks respectively.

2.3 T cell CAR Transduction

2.31 Phoenix A Cell Transfection

Phoenix A cells were transfected when they reached appropriate confluency (between 50-80%). 3µg or 9µg of the retroviral vector pCL ampho [Imgenex, San Diego, USA] was used to stimulate retroviral virion release from Phoenix A cells. pCL ampho plus 3µg or 9µg of the CLEC14a specific second generation CAR plasmid DNA (CRT3) [produced by Zhuang, X.] were added to 600µl or 1800µl of Optimem [Gibco, UK], followed by 24µl or 72µl of PEI stock (1mg/ml) [Sigma-Aldrich, Gillingham, UK] for each T25 or T75 flask of Phoenix A cells respectively. For mock transfection of Phoenix A cells no DNA was added. Transfection products were mixed by gentle vortexing and left to form DNA/PEI complexes for 10 minutes at room temperature. Media was gently removed from the Phoenix A cells and replaced with 3.5mls or 10.5mls of fresh transfection media for a T25 or T75 flask respectively. DNA/PEI complexes were gently added to the transfection media of Phoenix A flasks and mixed by north-south and east-west movements of the flask. Phoenix A cells were

incubated for 24 hours at 37°C/ 5% CO2, before transfection media was replaced with fresh transfection media and incubated for a further 24 hours at 37°C/ 5% CO_2.

2.32 Spinfection

2mls of retronectin (30µg/ml) [Clontech, Saint-Germain-en-Laye, France] was added to the required number of wells of a non-tissue-culture treated 6-well plate and incubated for 3 hours at room temperature. Retronectin was then removed and wells were blocked with 2.5mls of PBS + 2% BSA [Sigma-Aldrich, Gillingham, UK] for 30 minutes and then washed three times with 4mls of PBS. Phoenix A cell supernatants containing retrovirus were harvested and spun down at 400g for 5 minutes to pellet any suspended Phoenix A cells. 1.5mls of retroviral supernatant were added to the retronectin-coated wells and spun at 2000g for 120 minutes in a centrifuge prewarmed to 32°C. PBMCs and CBMCs were prepared for retroviral transduction by resuspending cells at $1x10^6$/ml in TCM plus IL-2 (100IU/ml) and incubating for 15 minutes at 37°C/5% CO_2 to allow cells to recover from centrifugation. When the spinfection was completed, retroviral supernatants were removed and wells washed once with PBS before PBMCs or CBMCs were added to the retrovirus-coated plate. The plate was then spun at 500g for 5 minutes and incubated at 37°C/5% CO_2. The following day, transduced cells were spun down at 500g for 5 minutes and resuspended in fresh TCM plus IL-2 (100U/ml) and placed in wells of a tissue culture-treated 6-well plate.

2.4 Cell Surface Fluorescent Antibody Staining

200µl of cells were transferred into individually labelled FACs tubes and spun at 600g for 4 minutes. Cells were washed once with 4mls of PBS and again spun at 600g for 4 minutes. Supernatants were poured off and 1.5µl of LIVE/DEAD fixable violet dead cell stain [Invitrogen, UK, #L34955] was added to the resuspended cell pellet and incubated for 20 minutes at room temperature in the dark. Cells were then washed with 4mls of cold MACs buffer and spun at 600g

for 4 minutes. Supernatants were poured off and fluorescently labelled cell surface antibodies were added at the required volumes (Table 1) and incubated for 30 minutes on ice in the dark. Cells were then washed twice with 4mls of cold MACs buffer and resuspended in 200µl of MACs buffer before being analysed on an LSR II multi-colour flow cytometer [BD]. Results were analysed using FlowJo software.

Table 1: List of Antibodies used for Cell Surface Staining

Name	Isotype	Company	Clone Number	Catalogue Number	Dilution
Pe Mouse Anti-human CD4	IgG1 κ	BD Biosciences	RPA-T4	555347	1:25
CD8 AmCyan	IgG1 κ	BD Biosciences	SK1	339188	1:20
Pe-Cy5-mouse Anti-human CD34	IgG1 κ	BD Biosciences	581	555823	1:40
CD45RA AlexaFluor 700 anti-human	IgG2b κ	Biolegend	HI100	304120	1:50
Anti h-CCR7 Fluorescein Conjugated Mouse IgG2a	IgG2a κ	R&D	150503	FAB197F	1:5
AlexaFluor 700 Mouse IgG2a Isotype Control	IgG2a κ	BD Biosciences	G155-178	557880	1:20
Mouse IgG2a FITC Isotype Control	IgG2a κ	BD Biosciences	X39	349051	1:1

2.5 IFN-γ Enzyme-Linked Immuno Sorbant Assay (ELISA)

A maxisorp 96-well plate (Nunc) was coated with either 50µl of PBS, human Fc fragment (1µg/ml) [Bethyl, Montgomery, USA] or human CLEC14A-Fc protein (1µg/ml)[produced by Zhuang, X.] diluted in sterile PBS in triplicates and incubated overnight at 2-8°C. The following day the wells were aspirated, washed with 200µl of ELISA media and 50µl of ELISA media was added to each well to prevent drying. PBMCs and CBMCs were fluorescently stained for CAR expression and $1x10^6$ CAR-transduced cells were counted and diluted with mock transduced cells so that all samples had the same proportion of transduced cells. Cells were spun at 500g for 5 minutes, the

supernatant discarded and resuspended in 500µl of ELISA media. 50µl of cells were added to each well to give a total volume of 100µl. The 96-well plate was spun at 400g for 3 minutes and incubated for 24 hours at 37°C/5% CO_2. On the same day another 96-well maxisorp plate was coated with anti-human IFN-γ antibody (0.75µg/ml)[Thermo Scientific, #M700A] diluted in coating buffer, sealed with nescofilm and incubated overnight at 2-8°C. The following day the anti-IFNγ antibody was flicked off and each well was blocked for 2 hours at room temperature with 200µl of blocking buffer. The plate was then washed four times with PBS/Tween20 using an automated plate washer and immediately 50µl of transduced PBMC or CBMC supernatants, or recombinant human IFNγ [Sigma-Aldrich, Gillingham, UK] standards at 0, 312.5, 625, 1250, 2500, 5000, 10000 and 20000pg/ml were added to the corresponding wells The plate was incubated at room temperature for 3 hours, washed four times with PBS/Tween20 and 50µl of biotinylated anti-IFNγ antibody (0.75µg/ml)[Thermo Scientific, #M701B] diluted in blocking buffer was added to each well. The plate was incubated for an hour and washed 4 times with PBS/Tween20. 50µl of extra-avidin peroxidase [Sigma-Aldrich, Gillingham, UK] diluted 1:1000 in blocking buffer was added to each well. The plate was incubated for 30 minutes and then washed 8 times with PBS/Tween20. 50µl of TMB substrate [Invitrogen, UK, #00-2023] was added to each well for 20 minutes before 50µl/well of 1M Phosphoric Acid was added to stop the reaction. The plate absorbance was then measured at 450nm on a plate reader [Biorad 680] and IFNγ concentrations determined from the IFNγ standard curve.

2.6 Statistical Analysis

A two-tailed unpaired T-test was used to compare the percentages of Tn and Tem cells within CAR-transduced CBMCs and PBMCs, and to compare their IFNγ responses to target antigen.

3.0 RESULTS

Successful CAR T cell transduction can be measured by analysing the cell-surface expression of a truncated CD34 molecule that is present in the CAR construct. CD34 expression was previously shown to accurately correlate with CAR expression (data not shown). PBMCs and CBMCs were both successfully transduced with the CRT3 second generation CAR targeting the tumour vasculature antigen CLEC14A. The cell-surface markers CCR7 and CD45RA have been shown to discriminate between differentiated T cell subsets, therefore the expression of these two markers was used to analyse cell populations [46].

3.1 Isotype-Control Staining

PBMCs and CBMCs were stained with the following panel of fluorescently labelled antibodies: CD4-Pe, CD8-AmCyan, CD34-PeCy5, CCR7-FITC and CD45RA-AF450. This allowed us to determine the differentiation phenotype of non-transduced and transduced PBMCs and CBMCs in both CD4+ and CD8+ T cells. In order to determine truly positive CCR7 and CD45RA staining both PBMCs and CBMCs were stained with isotype-control antibodies, specifically IgG2a FITC and IgG2a AF450 (Figure 1). Isotype-control staining was clearly negative for both CD4+ and CD8+ PBMCs and CBMCs, revealing no non-specific CCR7 and CD45RA background staining and this was seen in all samples analysed. Isotype-control staining was then performed on every sample analysed by flow cytometry in order to accurately determine the threshold for positive staining.

3.2 Differentiation Phenotype of Resting PBMCs and CBMCs

PBMCs and CBMCs were thawed and incubated in complete RPMI for 3 hours at 37°C to allow time for re-expression of cell-surface molecules before being stained for differentiation markers (Figure 2). Firstly, from analysing the forward and side scatter of the total cell populations it was

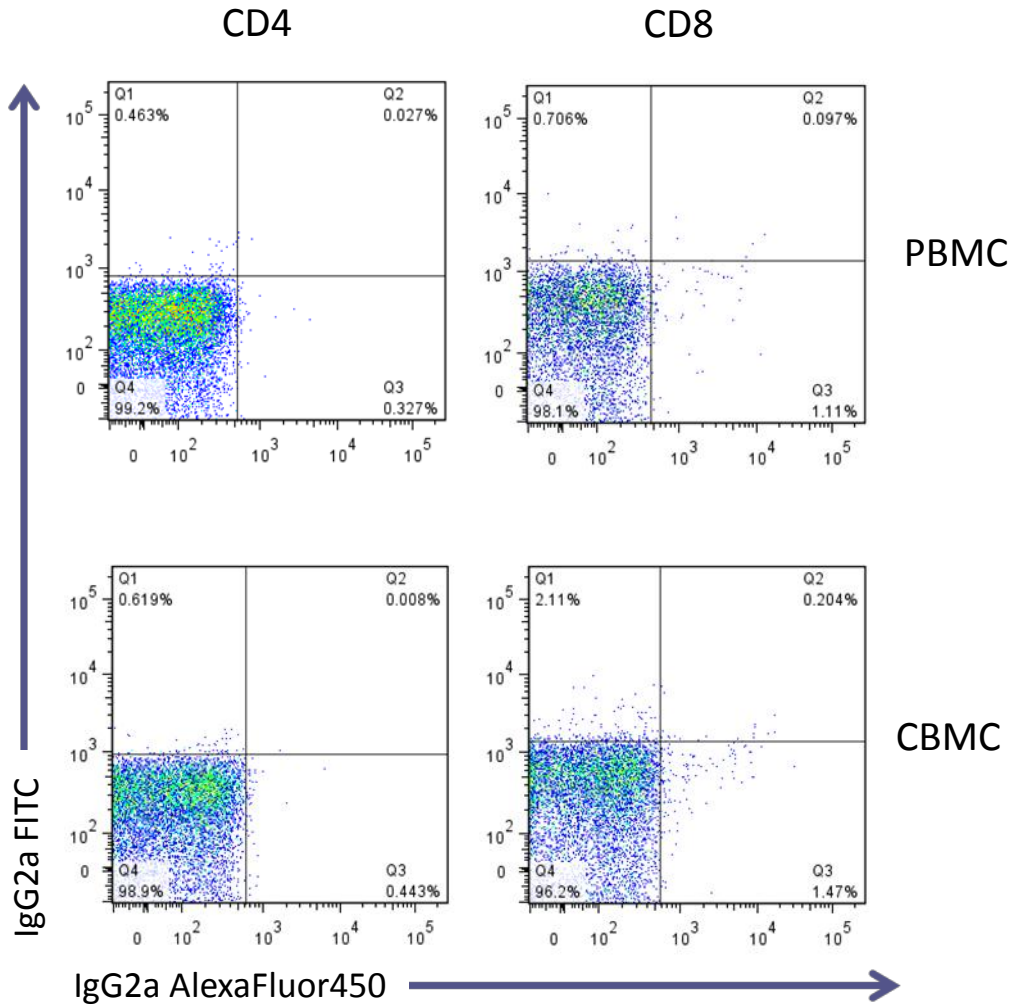

Figure 1| CCR7 and CD45RA Isotype Control Staining. To control for background FITC CCR7 and CD45RA AlexaFluor 450 staining, transduced PBMCs and CBMCs were stained with an IgG2a FITC and IgG2a AlexaFluor450 antibody. Data were gated on live lymphocytes detected using a vital dye and FSC:SSC profile. CD4 and CD8 T cells expressing CD34 were then analysed for isotype control staining. Negative staining of both PBMCs (top panel) and CBMCs (bottom panel) was seen in all cases. These are representative data from 7 PBMC and 9 CBMC independent experiments.

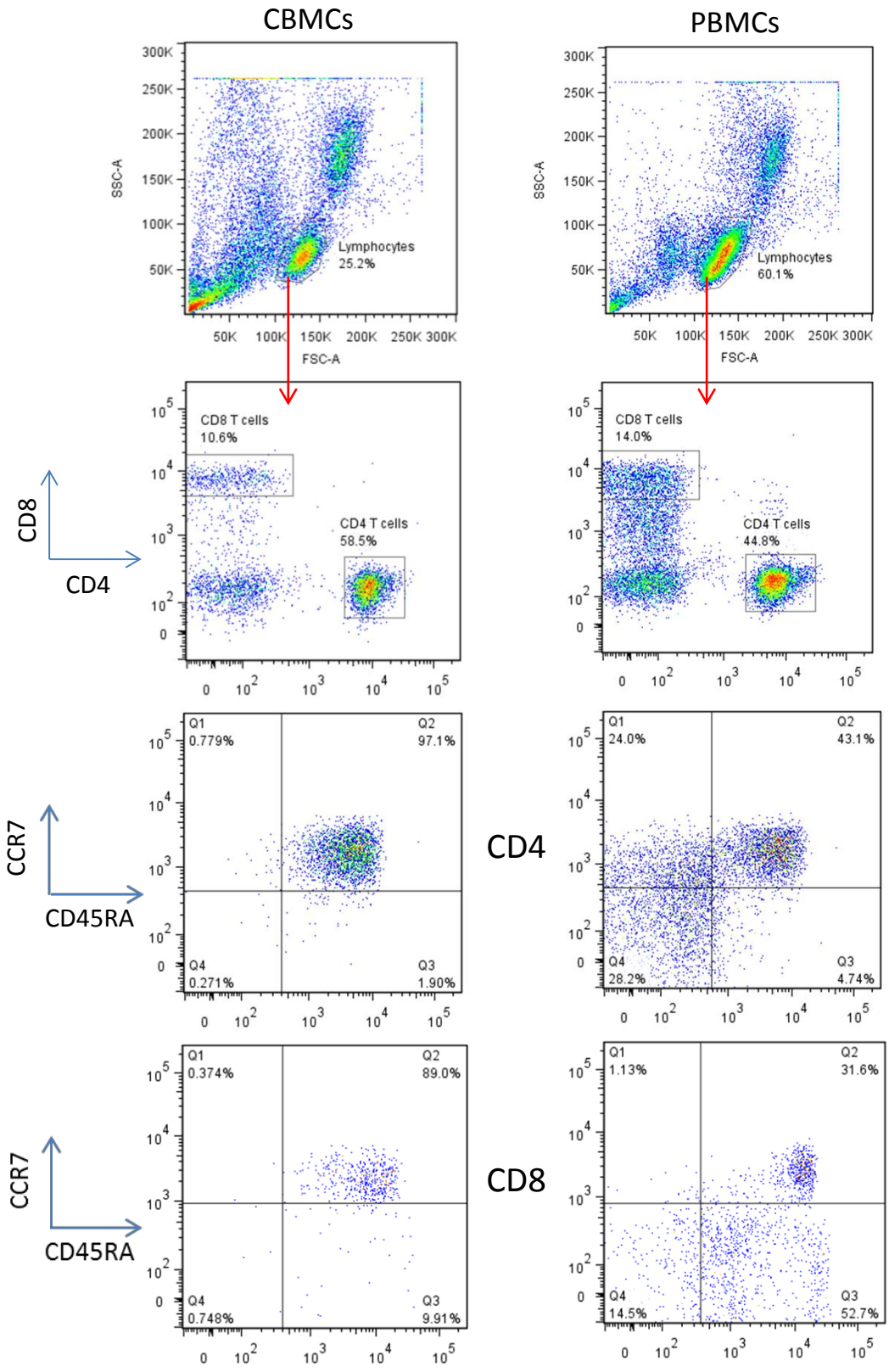

Figure 2|Differentiation Phenotype of Resting PBMCs and CBMCs. PBMCs and CBMCs were thawed and incubated for 2 hours in complete RPMI before being fluorescently stained for the differentiation markers. Data were gated on the lymphocyte population based on the FSC:SSC plot and the CD4 and CD8 T cell compartments analysed for CCR7 and CD45RA expression using gates determined by isotype control staining (n=1).

clear that CBMCs contain fewer live lymphocytes (25.2%) and more dead cells compared to that of PBMCs (60.1%). Secondly, after gating on the lymphocyte population the CD4/CD8 T cells ratios appeared to be different for CBMCs and PBMCs (approximately 6:1 and 3:1 respectively). Thirdly, CBMCs and PBMCs displayed very different CCR7 and CD45RA expression profiles in both the CD4+ and CD8+ T cells. Nearly all CD4+ and a large majority of CD8+ CBMCs had a naïve $CCR7^{+}$ $CD45RA^{+}$ phenotype, an expected feature of CBMCs. In contrast, over 50% of CD4+ PBMCs had a non-naive central memory ($CCR7^{+}$ $CD45RA^{-}$), effector memory ($CCR7^{-}$ $CD45RA^{-}$) or revertant effector memory ($CCR7^{-}$ $CD45RA^{+}$) phenotype. CD8+ PBMCs contained approximately a third of naïve T cells and a moderate effector memory cell population, however also contained an unusually high population of revertant effector memory T cells that are thought to be the most terminally differentiated T cell.

3.3 Differentiation Phenotype of PBMCs and CBMCs Transduced with a CAR

PBMCs and CBMCs were retrovirally transduced with the CAR construct and analysed for differentiation markers four days later. Representative results from 6 independent transductions are shown in Figure 3. Mock cells were handled in the same way but not exposed to a retroviral vector and therefore did not show any CD34/CAR expression. As expected, following activation of the T cells to permit retroviral transduction the majority of mock PBMCs had differentiated to an effector memory phenotype in both CD4+ and CD8+ T cells, while mock CBMCs are dominated by naïve T cells. The presence of so many naïve T cells suggests that CBMCs were not activated as well as PBMCs. CBMCs may have therefore been harder to transduce; however the average transduction rates were comparable between PBMCs and CBMCs (22.8% and 21.1% respectively; data not shown). By comparing these data to those obtained for resting cells (Figure 2) it is clear that the *in vitro* process of T cell activation drives the differentiation of T cells, but to a lesser

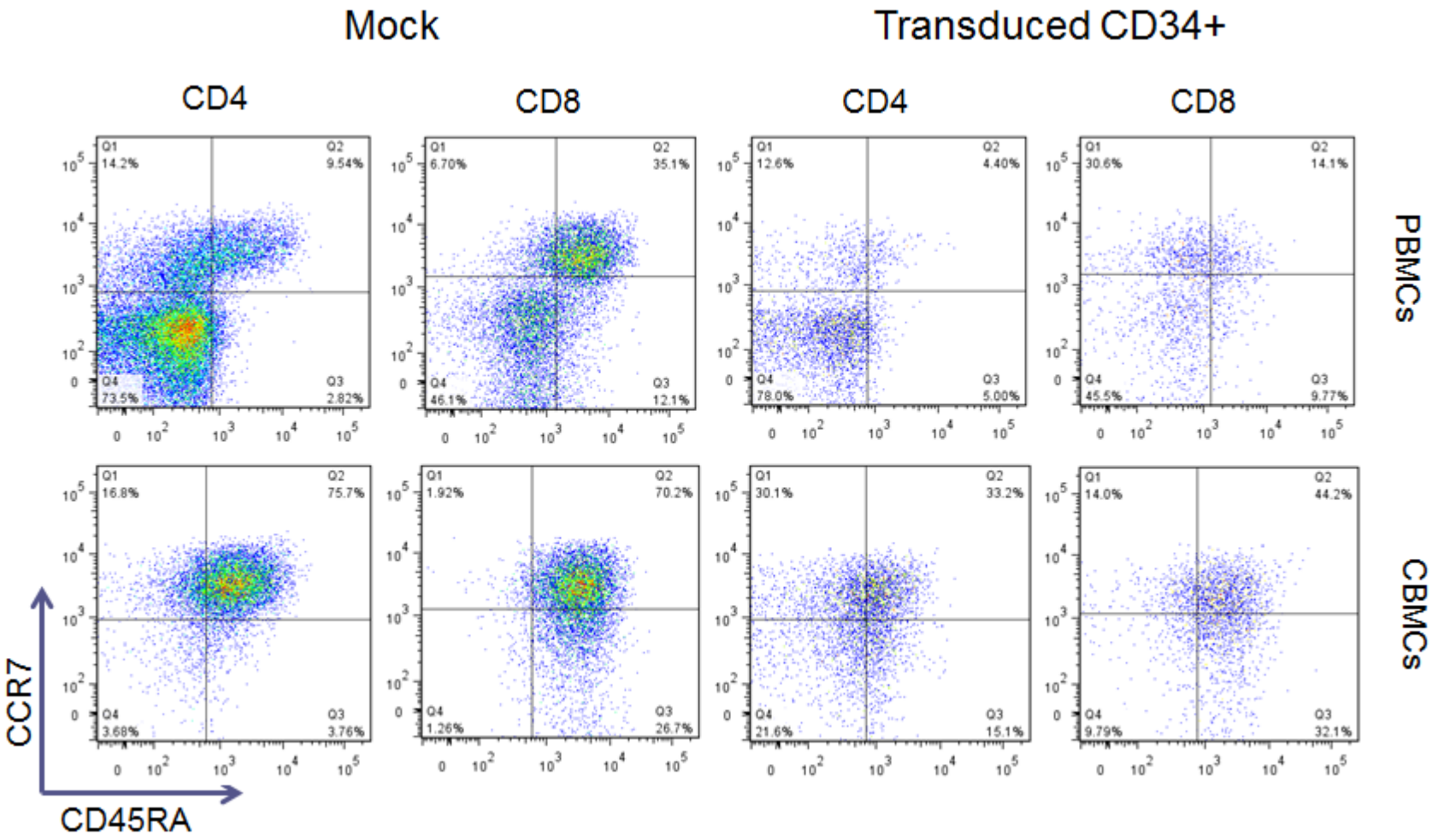

Figure 3| The Differentiation Phenotype of Transduced PBMCS and CBMCs. Both PBMCs and CBMCs were mock transduced and transduced with a CAR. Live lymphocytes were gated on and analysed for CD34 expression. The CD4 and CD8 compartments of mock and CD34+ transduced PBMCs and CBMCs were then analysed for CCR7 and CD45RA using gates determined by isotope control staining. These results are representative of 6 individual experiments.

degree in CBMCs. Interestingly, a high level of T_{EMRA} cells were observed in the CBMC mock CD8+ compartment. As T cells differentiate they are seen to move anticlockwise around a CD45RA Vs CCR7 plot, however in the case of CD8+ CBMCs it appears that at the time point analysed cells had not lost CD45RA expression before CCR7 expression. CAR expressing PBMCs and CBMCs were isolated by gating on positive CD34 expression. CD4+ and CD8+ transduced PBMCs exhibited a slightly more differentiated phenotype than mock cells as shown by an increase in Tem cell percentage and a slight decrease in Tn cell percentage. A more evident increase in Tem cells and decrease in Tn cells was seen in CD4+ and CD8+ CBMCs; however CBMCs still retain a less differentiated phenotype compared to PBMCs. Again transduced CD8+ CBMCs appeared to have an unusually high percentage of T_{EMRA} cells at the time point analysed.

The mean percentages of T cell subsets within PBMCs and CBMCs, taken from 7 PBMC and 9 CBMC independent transductions, are shown graphically in figure 4. This plainly shows that the majority of CD4+ PBMCs are Tem cells regardless of transduction. CRT3 transduced CD8+ PBMCs are also dominated by Tem cells, however mock and CRT3 non-transduced CD8+ PBMCs contained equal percentages of Tem and Tn cells. In contrast, CD4+ CBMCs were significantly dominated by less differentiated Tn and Tcm cells ($P<0.005$). CD4+ CRT3-transduced CBMCs contained a marginally smaller percentage of Tn cells and a larger percentage of Tem cells relative to those not expressing the CAR; however the percentage of the most differentiated effector and T_{EMRA} cells were significantly lower than in CD4+ CRT3-transduced PBMCs ($P=0.0001$). Mock and CRT3 non-transduced CD8+ CBMCs were also dominated by Tn cells but interestingly, CD8+ CRT3 transduced CBMCs on average contained similar percentages of all 4 T cell subsets. The percentage of Tn cells was found to be significantly higher in CD8+ CRT3-

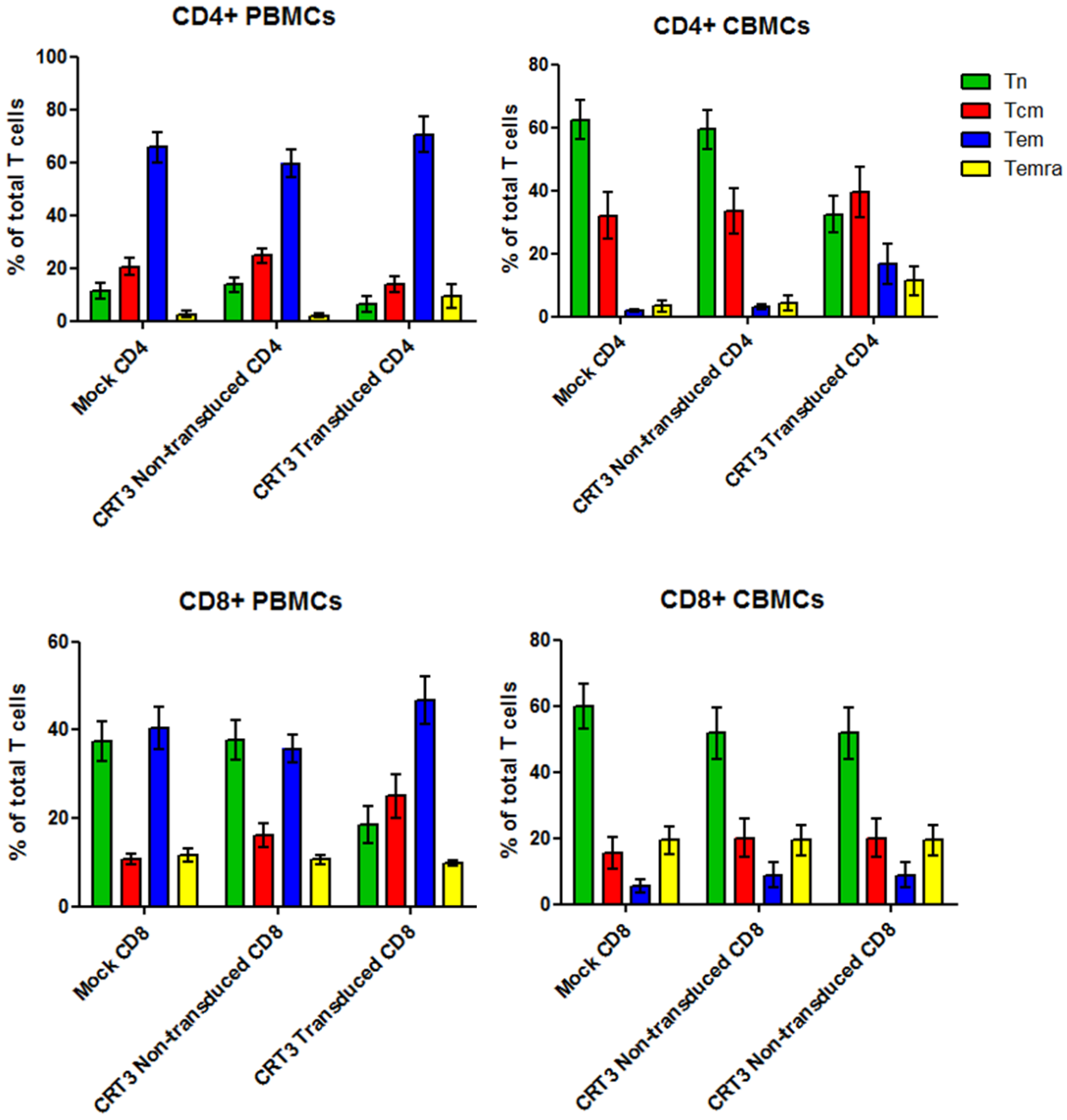

Figure 4| The Mean Percentages of T cell Subsets within PBMC and CBMC Populations. Mock transduced, CD34- CRT3 non-transduced and CD34+ CRT3 transduced PBMCs and CBMCs were analysed for differentiation markers using flow cytometry. The mean percentages of naïve (Tn), central memory (Tcm), effector memory (Tem) and reverter effector memory (Temra) T cells are shown for PBMCS (n=7) and CBMCs (n=9). Error bars represent the SEM.

transduced CBMCs compared to PBMCs (P=0.005), however the difference in percentage of effector and T_{EMRA} cells was found to not be statistically significant.

3.4 IFNγ Secretion by PBMCs and CBMCs Expressing the CRT3 CAR in Response to CLEC14A

The CRT3 CAR specifically targets the tumour vasculature antigen CLEC14A. Binding of CLEC14A protein to CRT3 expressed by transduced T cells should stimulate downstream T cell signalling and induce functional responses including the release of IFNγ. To test this IFNγ ELISA's were performed to quantify the IFNγ secretion in response to human CLEC14A protein (Figure 5). To control for non-specific IFNγ production responses to the Fc fragment present in the CAR construct and PBS used to coat the ELISA plate were also analysed. No substantial IFNγ secretions were observed by mock PBMCs and CBMCs in response to PBS, Fc or human CLEC14A. Large IFNγ secretions were observed by CRT3 transduced PBMCs from two donors in response to CLEC14A. An observable but significantly smaller IFNγ secretion was seen by CRT3 transduced CBMC donor 2 (P<0.0001), however no IFNγ secretion above the PBS and Fc threshold response was seen in CBMC donor 1. However, it is important to note that donor 1 CBMCs were in poor condition prior to the ELISA and it is therefore likely that a lot of CBMCs died during the experiment.

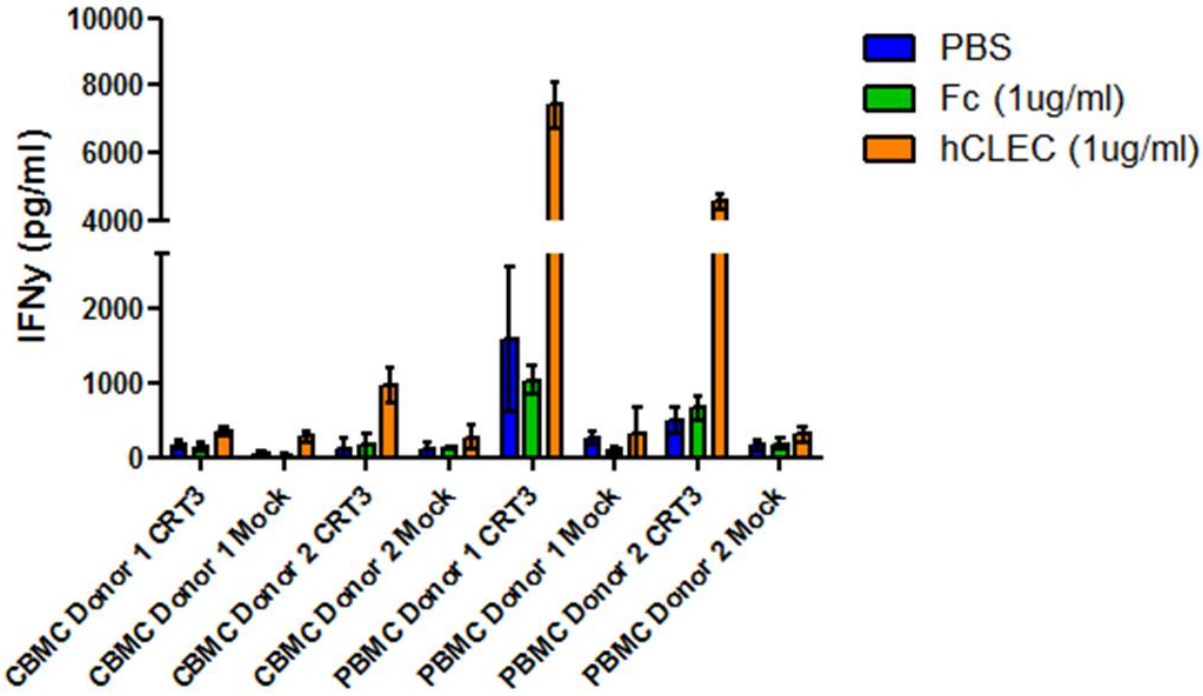

Figure 5| IFNγ ELISA of PBMCs and CBMCs. Mock and transduced PBMCs and CBMCs with equal transduction rates were incubated with PBC, Fc (1µg/ml) and human CLEC14A (1µg/ml) and the IFNγ responses were detected using an ELISA. The IFNγ response from CBMC donor 2 CRT3 cells was significantly lower than that of CRT3 PBMCs (P=0.0001). This figure represents the results from 3 independent experiments. The error bars represent the SEM.

4.0 DISCUSSION

This study has investigated the use of CBMCs as an alternative source of T cells for CAR-mediated anti-tumour ACT. Unlike PBMCs, CBMCs contain mostly undifferentiated naïve T cells. Less differentiated T cells have shown greater *in vivo* persistence and anti-tumour function, therefore CBMCs are an attractive source of T cells for ACT [37, 38].

4.1 Transduction of CAR-transduced PBMCs and CBMCs

CBMCs have previously been successfully genetically modified to express specific TCR genes [46]. The results from this study show that it is also possible to transduced CBMCs with specific CAR genes. Importantly, the level of expression of the CAR at the cell surface was indistinguishable to that of PBMCs therefore CBMCs are applicable for CAR-mediated ACT. Although, the lower overall percentage of lymphocytes within HUCB may mean a larger initial blood volume will be needed to generate sufficient numbers of CAR-T cells *in vitro*. The CBMCs utilised in this study had been freeze-thawed twice previously, therefore compromising their integrity and this is likely to account for the excess cell death seen in CBMC cultures. Isolating CBMCs from fresh HUCB may help solve this problem. HUCB banks are available that are not suitable for transplants but would provide enough CBMCs for ACT.

4.2 PBMC and CBMC Differentiation Following CAR gene Transfer

In agreement with Frumento *et al* (2012), it was shown that nearly all T cells in resting CBMCs have a naïve phenotype (Figure 2). This is an expected feature of CBMCs as they are not exposed to any pathogens *in utero* and therefore do not receive antigen stimulation. PBMCs on the other hand, are obtained from adult blood and so contain a much more diverse population of T cells including antigen experienced memory T cells due to infectious history. In addition, it was found that CBMCs

have a 2-fold higher CD4/CD8 T cell ratio compared to PBMCs which has also been reported by Harris e*t al* (1992). This characteristic could be beneficial to ACT as CD4 T cells can support and maintain the anti-tumour function of transduced CD8 T cells. Equally it may be disadvantageous as CD8+ T cells are more potent killers, therefore more testing would be required to determine if an increased CD4/CD8 T cell ratio is beneficial or not. A shortcoming of genetically engineering T cells however, is the need to activate cells prior to transduction to allow cell division and integration of the retroviral DNA. This *in vitro* process inevitably drives T cell differentiation which is not ideal for *in vivo* persistence and function. Lentiviral transduction does not require such extensive activation of T cells but cytokine activation is still necessary. Future studies need to compare transduction and differentiation of CBMCs using lentiviral transduction.

Indeed, the process of CAR transduction was shown to drive CBMC and PBMC T cell differentiation, shown by an increase in effector memory T cells and a decrease in naïve T cells (Figure 3, 4). After activation of PBMCs and CBMCs with anti-CD3 and IL-2, all cells displayed some degree of differentiation regardless of successful transduction of the CAR. As all cells were cultured and activated in identical conditions this was expected. The percentage of T cell subsets obtained for mock-transduced and non-transduced PBMCs and CBMCs were highly comparable, whereas CAR-transduced PBMCs and CBMCs showed a more differentiated phenotype, which was more obvious in CBMCs. It was hypothesised that mock-transduced and CAR-transduced T cells would have a similar more differentiated phenotype as this is needed for successful transduction. In addition, non-transduced cells might be predicted to be less differentiated as this would correlate with a less activated state and therefore less susceptible to retroviral transduction. However, these results suggest that expression of the CAR at the T cell membrane drives differentiation further than activating the cell alone (i.e. mock-transduction). This could be a result

of the physical insertion of the CAR construct into the T cell membrane. This disruption may increase downstream TCR signalling as the CAR contains a CD3ζ signalling domain, which is essential for propagating T cell activation signals.

Although differentiation was induced more in CAR-transduced CBMCs, cord-derived T cells still significantly retained a less differentiated phenotype compared to PBMCs, with approximately twice as many naïve cells and four times fewer effector memory cells (Figure 4). CBMCs have also been shown to retain a less differentiated phenotype after transduction of TCR genes specific for EBV [46]. These results support the use of CBMCs for CAR-mediated ACT over PBMCs due to their naïve phenotype. Frumento *et al* (2013) characterised TCR-modified CBMCs and PBMCs after antigen stimulation via SSC peptide-pulsed autologous dendritic cells to model *in vivo* antigen encounter, and found that after 23 days a difference in differentiation phenotype still existed. Effector memory T cells dominated the CBMC population whereas T_{EMRA} cells dominated the PBMC population. This process clearly drives T cell differentiation even further resulting in the majority of initially naïve CBMCs becoming effector memory T cells which is likely to limit their anti-tumour effects. Interestingly, it has been shown that the presence of IL-7 enhances the survival of naïve T cells *in vitro* [47] and *in vivo* [48]. The culture and expansion of genetically modified cells in the presence of IL-7 could therefore help maintain a less differentiated phenotype and help improve persistence and anti-tumour function in ACT.

4.3 TEMRA Staining

After antigen-stimulation of TCR-transduced CBMCs, Frumento *et al* (2012) found very few T_{EMRA} cells present. In contrast they found that PBMCs were dominated by T_{EMRA} cells after antigen-stimulation. As T_{EMRA} cells are thought to be the most terminally differentiated T cell subset it is not surprising that after 23 days of culture and antigen stimulation the majority of PBMCs had this

phenotype. In this current study an unusually high percentage of T_{EMRA} cells were found within CD8+ CBMCs, particularly CAR-transduced cells (Figure 4). A higher percentage of T_{EMRA} cells were also found within CD8+ PBMCs when compared to CD4+ T cells but markedly less than CBMCs. While the frequency of T_{EMRA} cells was high, the frequency of effector memory cells was low, which was unexpected as it is thought that T cells progressively differentiate through T cell subsets before regaining CD45RA expression and becoming terminally differentiated T_{EMRA} cells. It is possible that CD8+ CBMCs do not follow this same pattern of T cell differentiation, or that they do not lose CD45RA expression before CCR7 expression therefore move "clock-wise" around a CCR7 Vs CD45RA plot unlike the accepted anti-clockwise shift seen in PBMCs. It is also possible that at the time of phenotype analysis T_{EMRA} CD8+ CBMCs had already progressed through central and effector memory phenotypes and analysis was performed too late to observe this. Finally, it is possible that non-specific CD45RA staining accounted for the high frequency of T_{EMRA} cells. Although isotype control staining was negative for both CD4+ PBMCs and CBMCs, CD8+ T cells in particular did show a small amount of non-specific staining. Consequently it is unclear if the unusually high T_{EMRA} populations observed are true T_{EMRA} cells or artefacts.

4.4 Functionality of CAR-transduced PBMCs and CBMCs

The production of IFN-γ in response to CLEC14A antigen stimulation was investigated to assess the functionality of CAR-transduced PBMCs and CBMCs. CAR-transduced CBMCs were shown to produce only a moderate level of IFN-γ in comparison to CAR-transduced PBMCs (Figure 5). Although it is essential for transduced cells to sufficiently respond to target antigen, this observation was expected as CBMCs contained mostly naïve T cells that are yet to acquire effector functions such as IFNγ production. Based on data from Frumento *et al* (2012) and Serrano *et al* (2006), it is more than likely that after one or two rounds of antigen stimulation in culture, CAR-

transduced CBMCs would be able to produce IFNγ at similar levels to CAR-transduced PBMCs. Additionally, it has been shown that T cells that perform worse in *in vitro* functional assays actually have better *in vivo* function [28, 30]. Restifo *et al* (2005) found that IFNγ release and cytotoxicity assays negatively correlated with tumour regression in a mouse model. They hypothesised that this was because highly differentiated effector T cells were no longer 'fit' to proliferate and survive *in vivo,* and had exhausted their anti-tumour capabilities. They also reported that an increased T cell telomere length consistently defined increased persistence and tumour regression *in vivo,* and so was a superior method to evaluate ACT suitability. Therefore, although CAR-transduced CBMCs were seen to be inferior in this *in vitro* assay they may hold greater potential for tumour regression *in vivo.*

CBMCs have been transduced with a CAR recognising CD19 and these mediated CD19-specific cytolytic activity both in vitro and in vivo [49]. Notably, the phenotypes of CBMCs and PBMCs after genetic engineering were found to be similar in that the majority of cells had a CD8+ CD45RA- CCR7- effector memory phenotype. These results are different to those collected in this study, but are likely due to the *in vitro* propagation of CAR-transduced T cells for 10 weeks before phenotype analysis. Following these promising results, a phase I clinical trial is currently on-going to test the safety of a CD19-specific allogeneic umbilical cord blood cell infusion for patients with advanced B cell lymphomas (ID:NCT01362452).

4.5 Conclusions

The aim of this study was to compare the differentiation phenotypes and functionality of CAR-transduced PBMCs and CBMCs. This study has concluded that CBMCs retain a significantly less differentiated phenotype compared to PBMCs after CAR gene transfer. It has also concluded that CAR-transduced CBMCs produce significantly less IFNγ in response to target antigen compared to

PBMCs, a feature that may correspond to improved anti-tumour function in vivo. Therefore, my data suggest CBMCs are an attractive source of T cells for ACT using engineered effectors.

5.0 FUTURE WORK

The key to successful ACT for cancer is to achieve targeted potent anti-tumour cytotoxicity *in vivo.* In order to accurately assess the function of CAR-transduced CBMCs following antigen stimulation, more research needs to be carried out. Future work would include additional *in vitro* T cell effector function experiments. These could include CFSE-dilution proliferation assays, chromium-release cytotoxicity assays, video time-lapse microscopy to visualise cytotoxicity in real-time, intracellular fluorescent antibody staining for effector cytokines such as IFNγ, TNF and IL-2 as well as cell-surface staining for the T cell senescence markers KLRG-1 and CD57, and determining telomere length. Of note, in this study a CSFE-dilution proliferation assay was performed on CAR-transduced PBMCs and CBMCs, however by this stage the cells had been cultured for too long and were not in good enough condition to give clear data. It would also be important to study the effect of antigen encounter on CBMC differentiation *in vitro* using autologous cells expressing CLEC14A, and how the addition of IL-7 could help maintain a more naïve phenotype. Fundamentally, the *in vivo* toxicity and function of CAR-transduced CBMCs and PBMCs would need to be compared using an animal tumour-model. The expansion and persistence of infused cells would be measured using IVIS *in vivo* imaging of fluorescently labelled cells, and tumour regression would be a marker of *in vivo* anti-tumour function.

6.0 BIBLIOGRAPHY

[1] Collins, K., Jacks, T. and Pavketich, NP. (1997). The Cell Cycle and Cancer. *PNAS*, 94(7):2776-2778.

[2] Smith, A., Roman, E., Howell, D., Jones, R., Patmore, R. and Jack, A. (2009). The Haematological Malignancy Research Network (HMRN): a new information strategy for population based epidemiology and health service research. *British Journal of Haematology*, 148(5): 739-753.

[3] Gratwohl, A. *et al* (2010). Hematopoietic Stem Cell Transplantation – A Global Perspective. *Journal of American Medical Association*, 303(16):1617-1624.

[4] Weiden, PL., Flournoy, N., Thomas, D., Prentice, R., Fefer, A., Buckner, D., and Storb, R.(1979). Antileukemic Effect of Graft-versus-Host Disease in Human Recipients of Allogeneic-Marrow Grafts. *New England Journal of Medicine*, 300:1068-1073.

[5] Bleakley, M. and Riddell, S. (2004). Molecules and Mechanisms of Graft-Versus-Leukaemia Effect. *Nature Reviews Cancer*, 4: 371:380.

[6] Zhang, L., Conejo-Garcia, JR., Katsaros, D. *et al* (2003). Intratumoral T cells, recurrence, and survival in epithelial ovarian cancer. *New England Journal Medicine*, 348:203–13.

[7] Rosenberg, SA. and Dudley, ME. (2009). Adoptive cell therapy for the treatment of patients with metastatic melanoma. *Current Opinion Immunology*, 21:233–40.

[8] Gattinoni, L., Powell, DJ., Rosenberg, SA. and Restifo, NP. (2006). Adoptive immunotherapy for cancer: building on success. *Nature Reviews Immunology*, 6: 383-393.

[9] Dudley, ME., Wunderlich, JR., Robbins, PF., Yang, JC., Hwu, P., Schwartzentruber, DJ., Topalian, SL., Sherry, R., Restifo, NP., Hubicki, AM., Robinson, MR., Raffeld, M., Duray, P., Seipp, CA., Rogers-Freezer, L., Morton, KE., Mavroukakis, SA., White, DE. and Rosenberg, SA. (2002). Cancer regression and autoimmunity in patients after clonal repopulation with antitumor lymphocytes. *Science*, 298(5594): 850-4.

[10] Rosenberg, SA., Yannelli, JA., Yang, JC., Topalian, SL., Schwartzentruber,DJ., Weber, JS., Parkinson, DR., Seipp, CA., Einhorn, JH and White DE. (1994). Treatment of Patients with Metastatic Melanoma with Autologous Tumor-Infiltrating Lymphocytes and Interleukin 2. *JNCI J Natl Cancer Inst*, 86 (15): 1159-1166

[11] Berry, LJ., Moeller, M. and Darcy, PK. Adoptive immunotherapy for cancer: the next generation of gene-engineered immune cells. *Tissue Antigens,* 74: 277–289.

[12] Smith-Garvin, JE., Koretzky, GA. and Jordan, MS. (2009). T Cell Activation. *Annual Reviews Immunology*, 27: 591–619.

[13] Brentjens, RJ. and Curran, KJ. (2012). Novel cellular therapies for leukemia: CAR-modified T cells targeted to the CD19 antigen. *Haematology*: 143-152.

[14] Bendle, GM., Linnemann, C., Hooijkaas, AL., Bies, L., de Witte, MA., Jorritsma, A., Kaiser ADM., Pouw, N., Debets, R., Kieback, E., Uckert, W., Song, J., Haanen, J. and Schumacher, T. (2010). Lethal graft-versus-host disease in mouse models of T cell receptor gene therapy. Nature Medicine, 16: 565–570.

[15] Kuball,J., Dossett, Michelle L; Wolfl, Matthias; Ho, William Y; Voss, Ralf-Holger H; Fowler, Carla; Greenberg, Philip D (2007). Facilitating matched pairing and expression of TCR chains introduced into human T cells. *Blood*, 109: 2331-2338.

[16] Morgan, R., Dudley, M., Wunderlich, J., Hughes, M., Yang, J., Sherry, R., Royal, R., Topalian, SL., Kammula, U., Restifo, NP., Zheng, Z., Nahvi, A., de Vries, C., Rogers-Freezer, LJ., Mavroukakis, SA. and Rosenberg, SA. (2006). Cancer Regression in Patients After Transfer of Genetically Engineered Lymphocytes. *Science*, 314(5796): 126-129.

[17] Gross, G., Waks, T. and Eshhar, Z.(1989). Expression of immunoglobulin-T-cell receptor chimeric molecules as functional receptors with antibody-type specificity. *Proc Natl Acad Sci USA*, 86: 10024–10028.

[18] Riddell, SR., Jensen, MC. and June, CH. (2013). Chimeric Antigen Receptor Modified T Cells – Clinical Translation in Stem Cell Transplantation and Beyond. *Biology of Blood and Marrow Transplantation.* DOI: 10.1016/j.bbmt.2012.10.021

[19] Kowolik, CM., Topp, MS., Gonzalez, S. *et al*. (2006). CD28 costimulation provided through a CD19-specific chimeric antigen receptor enhances in vivo persistence and antitumor efficacy of adoptively transferred T cells. *Cancer Research*, 66(22):10995-11004.

[20] Kalos, M., Levine, BL., Porter, DL., *et al* (2011). T cells with chimeric antigen receptors have potent antitumor effects and can establish memory in patients with advanced leukemia. *Sci Transl Med*, 3: 95ra73.

[21] Maher, J., Brentjens, R., Gunset, G., Riviere, I. and Sadelain, M. (2002). Human T-lymphocyte cytotoxicity and proliferation directed by a single chimeric TCRzeta /CD28 receptor. Nature Biotechnology, 20(1): 70-5.

[22] Zhao, Y., Wang, Q., Yang, S., Kochenderfer, J., Zheng, Z., Zhong, X., Sadelain, M., Eshhar, Z., Rosenberg, S. and Morgan, R. (2009). A Herceptin-based Chimeric Antigen Receptor with Modified Signaling Domains Leads to Enhanced Survival of Transduced T lymphocytes and Antitumor Activity. Journal of immunology, 183(9): 5563-74.

[23] Zhong, X., Matsushita, M., Plotkin, J., Riviere, I. and Sadelain, M (2010). Chimeric Antigen Receptors Combining 4-1BB and CD28 Signaling Domains Augment PI3kinase/AKT/Bcl-XL Activation and CD8+ T cell-mediated Tumor Eradication. Molecular therapy: the journal of the American Society of Gene Therapy, 18(2): 413-20.

[24] Wilkie, S., Picco, G., Foster, J., Davies, D., Julien, S., Cooper, L., Arif, S., Mather, S., Taylor-Papadimitriou, J., Burchell, J. and Maher, J. (2008). Retargeting of Human T cells to Tumor-associated MUC1: the Evolution of a Chimeric Antigen Receptor. Journal of immunology, 180(7): 4901-9.

[25] Linnemann, C., Schumacher, T. and Bendle, G. (2011) T-Cell Receptor Gene Therapy: Critical Parameters for Clinical Success. Journal of Investigative Dermatology, 131: 1806–1816.

[26] Kerkar, SP., Muranski, P., Kaiser, A., Boni, A., Sanchez-Perez, L., Yu, Z., Palmer, DC., Reger, RN., Borman, ZA., Zhang, L., Morgan, RA., Gattinoni, L., Rosenberg, SA., Trinchieri, G. and Restifo, NP. (2010). Tumor-Specific CD8+ T Cells Expressing Interleukin-12 Eradicate Established Cancers in Lymphodepleted Hosts. Cancer Research, (17): 6725-34.

[27]Kochenderfer, JN., Wilson, W., Janik, JE., Dudley, ME., Stetler-Stevenson, M., Feldman, SA., Maric, I., Raffeld, M., Nathan D., Lanier, BJ., Morgan, RA. and Rosenberg, SA. (2010). Eradication of B-lineage cells and regression of lymphoma in a patient treated with autologous T cells genetically engineered to recognize CD19. *Blood*, 116(20): 4099–4102.

[28]Rosenburg, SA *et al* (2013). Cancer Regression and Neurological Toxicity Following Anti-MAGE-A3 TCR Gene Therapy. *Journal of Immunotherapy*, 36(2):133-51.

[29]Rosenberg SA. *et al* (2011). T Cells Targeting Carcinoembryonic Antigen Can Mediate Regression of Metastatic Colorectal Cancer but Induce Severe Transient Colitis. *Molecular Therapy*, 19(3): 620–626.

[30] Morgan, R., Yang, J., Kitano, M., Dudley, M., Laurencot, C. and Rosenberg, S. (2010). Case Report of a Serious Adverse Event Following the Administration of T cells Transduced with a Chimeric

[31] Di Stasi, A. *et al* (2011). Inducible Apoptosis as a Safety Switch for Adoptive Cell Therapy. New England Journal of Medicine, 365: 1673-83.

[32] Ruoslahti, E. (2002). Specialization of Tumour Vasculature. *Nature Reviews Cancer*, 2: 83-89.

[33]Bicknell *et al* (2012). Identification and angiogenic role of the novel tumour endothelial marker CLEC14A. Oncogene, 31(3): 293-305.

[34]Rho, S., Choi, H., Min, J., Lee, H., Park, H., Park, H., Kim, Y. and Kwona, Y. (2011). Clec14a is specifically expressed in endothelial cells and mediates cell to cell adhesion. *Biochemical and Biophysical Research Communications*, 404: 103–108.

[35] Klebano, CA. Gattinoni, L. and Restifo, NP. (2012). Sorting Through Subsets: Which T-Cell Populations Mediate Highly Effective Adoptive Immunotherapy? Journal of Immunotherapy, 35:651–660.

[36]Gattinoni, L., Lugli, E., Ji, Y., Pos, Z., Paulos, CM., Quigley, MF., Almeida, JR., Gostick, E., Yu, Z., Carpenito, C., Wang, E., Douek, DC., Price ,DA., June CH., Marincola FM., Roederer, M. andRestifo, NP. (2011). A human memory T cell subset with stem cell–like properties. *Nature Medicine*, 17(10): 1290-7.

[37] Gattinoni, L., Zhong, X., Palmer, DC., Ji, Y., Hinrichs CS., Yu, Z., Wrzesinski, C., Boni, A., Cassard, L., Garvin, LM., Paulos, CM., Muranski, P. and Restifo, NP. (2009). Wnt signalling arrests effector T cell differentiation and generates $CD8^+$ memory stem cells. *Nature Medicine*, 7: 808–813.

[38]Hinrichs, C., Borman, Z., Cassard, L., Gattinoni, L., Spolski, R., Yu, Z., Sanchez-Perez, L., Muranski, P., Kern, S., Logun, C., Palmer, D. and Ji, Y. (2009). Adoptively transferred effector cells derived from naive rather than central memory CD8+ T cells mediate superior antitumor immunity. PNAS, 106(41): 17469-74.

[39] Gattinoni, L., Klebanoff, CA., Palmer, DC., Wrzesinski, C., Kerstann, K., Yu, Z., Finkelstein, SE., Theoret, M., Rosenberg, S. and Restifo, N. (2005). Acquisition of full effector function in vitro paradoxically impairs

the in vivo antitumor efficacy of adoptively transferred CD8+ T cells. *Journal of Clinical Investigation*, 115(6): 1616–1626.

[40] Hinrichs, CS., Borman, ZA., Cassard, L., Gattinoni, L., Spolski, R., Yu, Z., Sanchez-Perez, L., Muranski, P., Kern, SJ., Logun, C., Palmer, DC., Ji, Y., Reger, RN., Leonard WJ., Danner, RL., Rosenberg, SA. and Restifo, NP., (2009). Adoptively transferred effector cells derived from naïve rather than central memory $CD8^+$ T cells mediate superior antitumor immunity. *PNAS*, 106(41): 17469–17474.

[41] Harris, DT., Schumacher, MJ., Locascio, J., Besencon, FJ., Olson, GB., DeLuca, D., Shenker, L., Bard, J. and Boyse, EA. (1992). Phenotypic and functional immaturity of human umbilical cord blood T lymphocytes. *PNAS*, 89(21): 10006–10010.

[42] (1994). Proliferative and Cytotoxic Responses of Human Cord Blood T Lymphocytes Following Allogenic Stimulation. *Cellular Immunology*, 154: 14-24.

[43] Rocha, V., Labopin, M., Sanz, G., Arcese, W., Schwerdtfeger, R., Bosi, A., Jacobsen, N., Ruutu,T., de Lima, M., Finke, J., Frassoni, F. and Gluckman, E. (2004). Transplants of Umbilical-Cord Blood or Bone Marrow from Unrelated Donors in Adults with Acute Leukemia. *New England Journal of Medicine*, 351: 2276-85.

[44] Sato, K., Nagayama, H. and Takahashi, TA. (1999). Aberrant CD3- and CD28-Mediated Signaling Events in Cord Blood T Cells Are Associated with Dysfunctional Regulation of Fas Ligand-Mediated Cytotoxicity. *Journal of Immunology*, 162: 4464-4471.

[45] Popovic, M., Lange-Wantzin, G., Sarin, PS., Mann, D. and Gallo, RC. (1983). Transformation of human umbilical cord blood T cells by human T-cell leukemia/lymphoma virus. *PNAS*, 80(17): 5402–5406.

[46] Frumento, G., Zheng, Y., Aubert, G., Raeiszadeha, M., Lansdor, PM., Moss, P., Lee, SP. and Chen, FE. (2013). Cord Blood T Cells Retain Early Differentiation Phenotype Suitable for Immunotherapy After TCR Gene Transfer to Confer EBV Specificity. *American Journal of Transplantation*, 13(1): 45-55.

[47] Tan, J., Dudl, E., LeRoy, E., Murray, R., Sprent, J., Weinberg, K. and Surh, C. (2001). IL-7 is critical for homeostatic proliferation and survival of naıve T cells. PNAS, 98(15): 8732–8737.

[48] Schluns, K., Kieper, W., Jameson, S., and Lefrançois, L. (2000). Interleukin-7 mediates the homeostasis of naïve and memory CD8 T cells in vivo. Nature Immunology, 1(5): 426-432.

[49] Serrano, LM., Pfeiffer, T., Olivares, S., Numbenjapon, T., Bennitt, J., Kim, D., Smith, D., McNamara, G., Al-Kadhimi, Z., Rosenthal, J., Forman, SJ., Jensen, M. and Cooper, L., (2006). Differentiation of naive cord-blood T cells into CD19-specific cytolytic effectors for posttransplantation adoptive immunotherapy. *Blood*, 107: 2643-2652.